

Self-consistent formulations for stochastic nonlinear neuronal dynamics

Jonas Stapmanns^{1,2,*}, Tobias Kühn^{1,2,*}, David Dahmen¹,
Thomas Luu³, Carsten Honerkamp^{2,4}, and Moritz Helias^{1,2}

¹*Institute of Neuroscience and Medicine (INM-6) and Institute for Advanced Simulation (IAS-6) and JARA BRAIN Institute I,*

Jülich Research Centre, Jülich, Germany

²*Institute for Theoretical Solid State Physics,*

RWTH Aachen University, 52074 Aachen, Germany

³*Institut für Kernphysik (IKP-3), Institute for Advanced Simulation (IAS-4) and Jülich Center for Hadron Physics,*

Jülich Research Centre, Jülich, Germany and

⁴*JARA-FIT, Jülich Aachen Research Alliance - Fundamentals of Future Information Technology, Germany*

(Dated: December 15, 2024)

Abstract

Neural dynamics is often investigated with tools from bifurcation theory. However, many neuron models are stochastic, mimicking fluctuations in the input from unknown parts of the brain or the spiking nature of input signals. Such noise in the input, however, changes the dynamics with respect to the deterministic model. We formulate the stochastic neuron dynamics in the Martin-Siggia-Rose De Dominicis-Janssen (MSDRJ) formalism and present the fluctuation expansion of the effective action and the functional renormalization group (fRG) as two systematic ways to incorporate corrections to the mean dynamics and time-dependent statistics due to fluctuations in the presence of nonlinear neuronal gain. To formulate self-consistency equations, we derive a fundamental link between the effective action in the Onsager-Machlup (OM) formalism, which lends itself to direct physical interpretation, and the MSDRJ effective action, which is computationally advantageous. These results in particular allow the extension of the OM formalism to non-Gaussian noise. This approach naturally leads to effective deterministic equations for the first moment of the stochastic system; they explain how nonlinearities and noise cooperate to produce memory effects. Moreover, the MSDRJ formulation yields an effective linear system that has identical power spectra and linear response. Starting from the better known loopwise approximation, we then discuss the use of the fRG as a method to obtain self-consistency beyond the mean. We present a new efficient truncation scheme for the hierarchy of flow equations for the vertex functions by adapting the Blaizot, Méndez and Wschebor (BMW) approximation from the derivative expansion to the vertex expansion. The methods are presented by means of the simplest possible example of a stochastic differential equation that has generic features of neuronal dynamics.

* J. Stapmanns and T. Kühn contributed equally to this work

I. INTRODUCTION

Neuronal networks are interesting physical systems in various respects: they operate outside thermodynamic equilibrium [1], a consequence of directed synaptic connections that prohibit detailed balance [2]; they show relaxational dynamics and hence do not conserve but rather constantly dissipate energy; and they show collective behavior that self-organizes as a result of exposure to structured, correlated inputs and the interaction among their constituents. But their analysis is complicated by three fundamental properties: Neuronal activity is stochastic, the input-output transfer function of single neurons is non-linear, and networks show massive recurrence [3] that gives rise to strong interaction effects. They hence bear similarity with systems that are investigated in the field of (quantum) many particle systems. Here, as well, (quantum) fluctuations need to be taken into account and the challenge is to understand collective phenomena that arise from the non-linear interaction of their constituents. Not surprisingly, similar methods can in principle be used to study these two a priori distinct system classes [4–8].

But so far, the techniques employed within theoretical neuroscience just begin to harvest this potential. Here we will take essential steps towards this goal. Concretely, we adapt methods from statistical field theory and functional renormalization group techniques to the study of neuronal dynamics. Applied to neuronal networks, the approach ultimately allows the characterization of their collective states of activity and transitions between them. These methodological developments hence offer a deepened understanding of the mechanisms that are at work in neuronal networks, because they provide a bridge between the microscopic stochastic dynamics and effective descriptions with reduced complexity. Moreover, such tools provide quantitative methods to compute the statistical properties of neuronal activity.

The large number of synaptic inputs to each neuron in a network allows the application of mean-field theory [9–11] to explain many dynamical phenomena, among them first order phase transitions. The transition from the a quiescent to a highly active state in a bistable neuronal network is a prime example of a first order phase transition in neuronal networks [11]. The activation of attractors embedded into the connectivity of a Hopfield network is a second [12]. Mean-field analysis applied to multi-area networks with large numbers of populations [13] explains their multi-stability and constrains model parameters by requiring stability of the dynamics [14]. Combined with linear response theory, network fluctuations

can quantitatively be described in binary [15–17] and in spiking networks [18–23]. Also transitions into oscillatory states by Andronov-Hopf bifurcations are in the realm of linear response theory around a mean-field solution [24–27]. The complete characterization of the phase diagram of neuronal networks is a prerequisite to constrain the computational principles at work in such networks.

Second order phase transitions in neuronal networks are more challenging, because the behavior of the system is dominated by fluctuations on all length scales, so that mean-field theory and its systematic correction by loopwise expansion often break down [4]. But these transitions are highly interesting from a neuroscientific point of view, because networks then show large susceptibility to signals. Moreover, signatures of critical states are found ubiquitously in experiments: Parallel recordings in cell cultures [28] and in vivo [29] show power law distributions in the numbers of co-active neurons, suggestive of scale free dynamics. Critical states also have consequences for information processing: reservoir computing [30, 31] with random networks close to criticality indeed shows the highest computational performance [32], maximizing the wealth of transformations they perform.

Close to second order phase transitions, the method of choice is to compute the effective action by renormalization group techniques [33]. A particularly powerful implementation is the functional renormalization group (fRG) [34–36]. It has witnessed successes in condensed matter physics in problems ranging from classical and quantum critical phenomena over the explorations of the ground states of interacting many-body systems to the improved determination of effective model parameters from ab-initio theories. It systematically improves the physical description beyond mean-field theory by including fluctuations and by removing ambiguities.

To date, one of the most powerful and versatile sets of methods is available for neuronal networks of stochastic differential equations: The Martin-Siggia-Rose-De Dominicis-Janssen (MSRDJ) formalism [37–39] has been used to apply diagrammatic perturbation theory and systematic fluctuation expansions to neuronal networks [7, 8]. This formalism has in particular been applied to describe genuine non-equilibrium dynamics in physical systems [5], including disordered systems [40]. Combined with replica theory [41], it has recently been used to find an exact condition for the transition from regular to chaotic activity [42], to compute the memory capacity of driven random networks [43], and to study the effect of bi-directional connectivity [44, 45]. The current manuscript employs this formalism to illus-

trate its application for stochastic dynamical equations. In order to keep the focus on the conceptual side, we demonstrate all approaches by means of the simplest non-trivial example we can think of, a scalar ordinary stochastic differential equation with linear and quadratic right hand side and Gaussian noise.

In [Section II A](#), we shortly recapitulate the naive mean-field solution of a stochastic differential equation and introduce its Onsager-Machlup (OM) field theory. We motivate this formulation by demonstrating that it allows the definition of an effective potential which locally acts like an energy. Moving on to the MSRDJ-field theory, we review in [Section II B](#) the loop expansion, which allows practical calculations of probabilistic quantities, which then by construction are determined self-consistently on the level of the first moments. We then demonstrate how the effective actions of these two formulations are related, extend the definition of the OM effective action to case of non-Gaussian noise and discuss the meaning of escape paths in both formulations; in particular, we resolve contradictory statements in the literature as to when moments of response fields vanish. In [Section II C](#), it is outlined that the minimum of the effective action defines an effective, deterministic, non-Markovian system showing the same dynamics as the mean value of the stochastic process. Having this at hand, we show how fluctuations influence the relaxation back to baseline after a small perturbation. Finally, in [Section II D](#) we present the functional renormalization group as a method that allows the self-consistent treatment up to arbitrary order of the vertex functions. In particular, in [Section II D 1](#) we present a new interpretation of the BMW approximation within the formulation of a vertex expansion. We show that letting flow all terms of the bare action in this altered BMW-fRG-scheme leads to an improvement over the one-loop result. In [Section III](#) we discuss the presented concepts in comparison to other approaches and provide an outlook towards applications within theoretical neuroscience.

II. RESULTS

A. Effective action and effective potential

We here consider the following generic stochastic differential equation

$$dx(t) = f(x(t)) dt + dW(t), \tag{1}$$

where x could denote a magnetization, the firing rate or activity of a neuron or of a population of neurons, the concentration of some chemical substance, the number of animals that reproduce and die or the value of a stock [46–48]. We will focus on the neuroscientific interpretation, in which case we parameterize $f(x) = -x + Jg(x)$. We call J the synaptic weight of the self-feedback which is mediated by the nonlinearity $g(x)$, the gain function, which typically is a sigmoid. The explicit term $-x$ shall describe the leaky dynamics of neurons. We choose the stochastic increment $dW(t)$ as a centered Gaussian with first and second moments given by

$$\langle dW(t) \rangle = 0, \quad \langle dW(t)dW(s) \rangle = D\delta_{t,s}dt.$$

This article investigates a sequence of approximation techniques to compute the statistics of the system self-consistently. We present methods with increasing complexity and accuracy, starting with the simplest possible self-consistent approximation: the neglect of fluctuations altogether.

Mean-field approximation The simplest self-consistent approximation of the statistics of the system consists of an ad hoc approach to the stochastic differential equation (1) that neglects the noise and instead solves the ordinary differential equation

$$\frac{d}{dt}x(t) = f(x(t)). \quad (2)$$

Finding the stationary solution to this differential equation amounts to a fixed point problem, that is $f(x_0) = 0$. Small fluctuations around that solution can, to first approximation, be accounted for by linearizing (1) around x_0 . By writing $x(t) = x_0 + \delta x(t)$, we obtain

$$\frac{d}{dt}\delta x(t) = f'(x_0)\delta x(t) + \xi(t) + \mathcal{O}(\delta^2 x(t)), \quad (3)$$

where ξ is a centered Gaussian white noise with variance D (formally the derivative of dW). Denoting the Fourier transform of x as X , we describe the first and second order statistics of these small fluctuations as

$$\begin{aligned} 0 = \langle \delta X(\omega) \rangle &= \frac{\langle \xi(\omega) \rangle}{i\omega - f'(x_0)}, \\ \langle \delta X(\omega) \delta X(\omega') \rangle &= \frac{2\pi D \delta(\omega + \omega')}{(i\omega - f'(x_0))(i\omega' - f'(x_0))}. \end{aligned} \quad (4)$$

This approach is, however, restricted to small noise amplitudes, and cannot be straightforwardly generalized.

From a conceptual point of view, this approximation is also not self-consistent, because we solve the deterministic equation (2) to determine the first moment x_0 and then study fluctuations around it to determine the second order statistics as (4). Such fluctuations would, in turn, affect the mean value, due to the non-linear parts of f . Continuing the Taylor expansion of f in (3) to second order, this ad hoc approach would then yield a correction to the mean given by $\langle x \rangle \simeq x_0 + \frac{1}{2} f''(x_0) \frac{D}{-2f'(x_0)}$, because the variance of the process, by (4), is $\langle \delta x^2 \rangle = \frac{D}{-2f'(x_0)}$. Thus we get an approximation for the mean that is inconsistent with the value x_0 that we assumed to perform the approximation in the first place. The common thrust of the methods surveyed in the remainder of this article is to strive for self-consistency of the statistics and to systematically compute such fluctuation corrections that are self-consistent also on the level of higher moments.

Path-integral formulation To study the system more systematically, we introduce the path integral formalism, starting with its Onsager-Machlup (OM) formulation [49, 50]. We assign a probability $p[x] \mathcal{D}x$ to every path $x(t)$, where we define the integral measure $\mathcal{D}x$ as

$$\int \mathcal{D}x \dots := \lim_{N \rightarrow \infty} \int dx_{t_0} \dots \int dx_{t_{N-1}} \dots,$$

where t_0, \dots, t_{N-1} is a uniform discretization of the time axis. We here stick to the Ito convention, which means that we evaluate the integrand at the beginning t_i of every subinterval $[t_i, t_{i+1})$. For additive noise as it appears in (1), all choices for a discretization converge to the same limit [51, chap. 4.3.6.]. Furthermore, we define $p[x] = \frac{1}{\mathcal{Z}} \exp(S_{\text{OM}}[x])$ via

$$\begin{aligned} S_{\text{OM}}[x] &= -\frac{1}{2} \lim_{N \rightarrow \infty} \sum_{i=0}^{N-1} \left(\frac{x_{i+1} - x_i}{\Delta t} - f(x_i) \right)^T D^{-1} \left(\frac{x_{i+1} - x_i}{\Delta t} - f(x_i) \right) \Delta t \\ &= -\frac{1}{2} \int dt (\partial_t x - f(x(t)))^T D^{-1} (\partial_t x - f(x(t))). \\ &= - \int dt L(x(t), \dot{x}(t)), \end{aligned} \tag{5}$$

[49, 50, 52, 53][54] and

$$\mathcal{Z}^{-1} := \int \mathcal{D}x \exp(S_{\text{OM}}[x])$$

is chosen such that the probability $p[x]$ is properly normalized. The probability of the occurrence of deviations from the solution fulfilling $\partial_t x = f(x)$ are suppressed exponentially. Therefore this solution is the most probable one - it is, however, not necessarily equal to the average

$$\langle x(t) \rangle := \int \mathcal{D}x p[x] x(t).$$

This average can be expressed as the functional derivative with respect to $j(t)$ of the moment-generating functional

$$Z[j] := \int \mathcal{D}x p[x] \exp\left(\int dt j(t) x(t)\right), \quad (6)$$

evaluated at $j(t) = 0$. Higher moments are obtained analogously by differentiating more often, so that Z contains the full information about the system. The cumulant generating function (or Helmholtz free energy) $W = \ln Z$ encodes the statistics in terms of cumulants, i.e. the derivatives of W , which is more efficient in the sense that higher order cumulants do not contain information already contained in lower orders.

In the following we review some central results that show the relation between the two commonly used path integral representations, the Onsager-Machlup formulation and the Martin-Siggia-Rose-De Dominicis Janssen formulation. Subsequently, we derive a novel relation between the corresponding effective actions. We also refine the consideration of non-zero response fields for cases of escape paths - solutions of the stochastic differential equation that are only enabled by the presence of the noise.

Most likely paths - Lagrangian formulation We would like to know the most probable path that connects an initial point $x(0) = x_0$ with a final point at $x(T) = x_T$. Because the form of the Onsager-Machlup action (5) is an integral over a Lagrangian L , a function of x and \dot{x} , the most likely path must obey an Euler-Lagrange equation, which results from a variation with fixed end points, as in classical mechanics (see [Section IV A](#), eq. (49)). For the stochastic differential equation (1), it takes the form

$$\ddot{x} = f(x) f'(x). \quad (7)$$

We see from the specific form of the Onsager-Machlup action (5) that the classical noise-less solution

$$\partial_t x = f(x) \quad (8)$$

solves (7) and in particular makes $S_{\text{OM}}[x]$ vanish; due to the positiveness of L , the solution (8) is also a minimum of L . If the initial point $x_0 \neq \bar{x}$ is in the basin of attraction of a fixed point \bar{x} of the deterministic equation, $f(\bar{x}) = 0$, then x relaxes towards \bar{x} and reaches x_T at time T . But (7) has a time-reversal symmetry: If $x(t)$ minimizes L between 0 and T , so does $y(t) := x(T - t)$. So inverting the direction of motion, we obtain a solution that starts

at x_T at 0 and moves to x_0 at time T . This solution is hence the most likely escape path for the given pair of end points, satisfying

$$\partial_t y = -f(y). \quad (9)$$

We use the term “escape path” for a trajectory that is only possible by the presence of noise.

Most likely paths - Hamiltonian formulation We may instead choose a Hamiltonian formulation by defining a new variable $\tilde{x} := \partial_{\dot{x}} L$, the response field, and the corresponding Hamiltonian by a Legendre transform

$$\begin{aligned} H[x, \tilde{x}] &= \sup_{\dot{x}} \dot{x} \tilde{x} - L(x, \dot{x}) \\ &= \tilde{x} f(x) - \tilde{x}^T \frac{D}{2} \tilde{x}. \end{aligned} \quad (10)$$

The supremum, using the non-negativeness of L , ensures the above definition of \tilde{x} . By the chain rule and the Euler-Lagrange equation, we obtain the pair of Hamiltonian equations (details in appendix [Section IV A](#), especially (49))

$$\dot{\tilde{x}} = -\partial_x H(x, \tilde{x}) = -\tilde{x} f'(x), \quad (11)$$

$$\dot{x} = \partial_{\tilde{x}} H(x, \tilde{x}) = f(x) - D\tilde{x}, \quad (12)$$

which are equivalent to (7). The linearity of the first equation always admits $\tilde{x} \equiv 0$ as a solution, corresponding to the most likely deterministic path (8) found above. This is in line with the noise having its maximal probability at a realization that vanishes for all time points. The time-reversed solution (9) here corresponds to the solution

$$\tilde{x} = \frac{2}{D} f(x), \quad (13)$$

because inserting the latter expression into (12) shows that it amounts to the reflection of time $t \rightarrow -t$; it is easily checked to satisfy (11), too. We therefore see that such an escape trajectory in general has a non-zero value of the response field \tilde{x} . In the literature various statements exist as to why all moments of the response field are supposed to vanish [55, 56]. However, we show in [Section IV B](#) that a nonzero response field is indeed compatible with the normalization of a path integral with fixed end points.

MSRDJ Formulation The Onsager-Machlup action (5) can, conversely to (10), be expressed as a Legendre transform of H as

$$\begin{aligned} L[x, \dot{x}] &= \sup_{\tilde{x}} \tilde{x} \dot{x} - H(x, \tilde{x}) \\ &= \sup_{\tilde{x}} \tilde{x} (\dot{x} - f(x)) + \tilde{x}^T \frac{D}{2} \tilde{x}. \end{aligned} \quad (14)$$

The latter yields the form of the Martin-Siggia-Rose-De Dominicis-Janssen (MSRDJ) action [37–39, 57], defined on the $2N$ -dimensional phase space as

$$S_{\text{MSRDJ}}[x, \tilde{x}] := \tilde{x}^T (\partial_t x - f(x)) + \tilde{x}^T \frac{D}{2} \tilde{x}, \quad (15)$$

where $x^T y = \int_{-\infty}^{\infty} x(t) y(t) dt$ denotes the inner product with respect to time. For Gaussian noise, we hence have the fundamental relation between the Onsager-Machlup and the MSRDJ action

$$S_{\text{OM}}[x] = \sup_{\tilde{x}} S_{\text{MSRDJ}}[x, \tilde{x}]. \quad (16)$$

Alternatively, one may obtain this result by performing a Hubbard-Stratonovitch transform, that is by using the identity $e^{-\frac{x^2}{2}} = \frac{1}{i\sqrt{2\pi}} \int_{-i\infty}^{i\infty} e^{\frac{\tilde{x}^2}{2} + \tilde{x}x} d\tilde{x}$ with the response field as an additional auxiliary variable \tilde{x} . The MSRDJ formulation has the advantage that only a single first order differential operator in time appears.

Stochastic dynamics as a variational problem It is beneficial to reformulate self-consistency equations as solutions to a variational problem. The reason is simple: If we find a functional $\Phi[x^*]$ that assumes stationary points $\Phi^{(1)}[\tilde{x}] = 0$ at the true mean value $\tilde{x}(t) \equiv \langle x(t) \rangle$, such an equation necessarily has the form of a self-consistency equation - its left hand side is a natural function of the mean, which will therefore necessarily appear on the right hand side, too. Indeed such a functional is readily defined as

$$\begin{aligned} \Gamma_{\text{OM}}[x^*] &:= \sup_j j^T x^* - W[j], \\ \Phi[x^*, j] &:= \Gamma_{\text{OM}}[x^*] - j^T x^*. \end{aligned} \quad (17)$$

The so-defined Γ_{OM} , the Legendre transform of W , is the effective action (or Gibbs free energy) [4]. It is central to the study of phase transitions, which reduces to finding the stationary points or regions of Φ [59, i.p. Chapter 6]. Such a formulation is in particular beneficial for the study of second order phase transitions, points in parameter space where

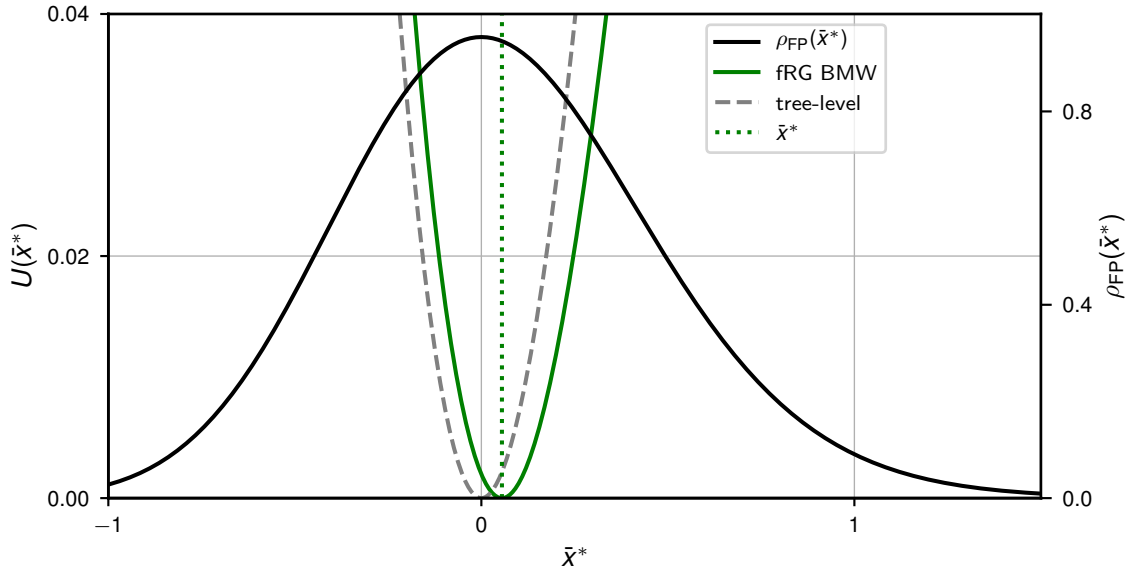


Figure 1. Effective potential $U(\bar{x})$, as defined in (26), in different approximations. Practically, we used (19) where we replaced the bare quantities by the corrected ones. The dashed line represents the tree-level approximation (19) and the solid line the fRG result with truncation after $\Gamma_{\bar{x}xx,\text{fl}}^{(3)}$, including the BMW approximation, see Section IID 1. The probability density obtained as the solution of the Fokker-Planck equation [58] is shown in black for comparison. The dotted line indicates the position of the mean value \bar{x} computed via the fRG calculation. Parameters for specific choice of $f(x)$, see (27): $l = 0.5$, $\beta = 0.15$, $D = 0.17$.

the first derivative $W^{(1)}[j]$ becomes multi-valued. At such points, Φ has a flat segment, but is continuously differentiable everywhere [60] and is thus analytically simpler than the non-analytical W . Another advantage is that symmetries of S_{OM} are also symmetries of Γ_{OM} , giving rise to Ward-Takahashi identities [61] and the study of Goldstone fluctuations in symmetry broken states of systems that admit a continuous symmetry.

The simplest approximation to the effective action is obtained in tree-level approximation. In correspondence to (2) we neglect all fluctuations and hence replace the integral over all configurations x in the definition of Z in (6) by its supremum, which yields $W[j] \simeq \ln \sup_x \exp(S_{\text{OM}}[x] + j^T x) - \ln \mathcal{Z}[0]$. The monotonicity of \exp and the involution property

of the Legendre transform (17) then yield

$$\Gamma_{\text{OM}}[x^*] \simeq -S_{\text{OM}}[x^*] + \text{const.} \quad (18)$$

Limiting the study to stationary solutions $\bar{x}^* := x^*(t) = \text{const.}$, such that $X(\omega) = 2\pi\delta(\omega)\bar{x}^*$, it is convenient to introduce a potential $U(\bar{x}^*)$ that is stationary precisely at the point that corresponds to the scalar mean value of the system.

In tree level approximation (18) and with (5) we have

$$U_0(\bar{x}^*) = \frac{1}{T}S_{\text{OM}}(\bar{x}^*) = \frac{1}{2TD} \int_0^T dt (-f(\bar{x}^*))^2 = \frac{1}{2D} (f(\bar{x}^*))^2, \quad (19)$$

where we introduced T as the total time during which we observe the system. If we neglect the noise, $U_0(\bar{x}^*) \propto \delta(\bar{x} - \bar{x}^*)$ because there are no fluctuations. For $D > 0$, the minimum of $U_0(\bar{x}^*)$ determines the mean value \bar{x} and its curvature at this minimum equals the inverse of the zero-frequency fluctuations $\langle X(0)^2 \rangle - \langle X(0) \rangle^2$ around the mean. We deduce this, using $f(\bar{x}) = 0$, from

$$U_0''(\bar{x}) = \frac{\partial^2}{\partial \bar{x}^{*2}} U_0(\bar{x}^*) \Big|_{\bar{x}} = \frac{(f'(\bar{x}))^2}{D},$$

compared to the covariance (4) in linear response. Observing that differentiating twice with respect to the zeroth Fourier mode yields the same number times a (maybe singular) generic factor, leads to the insight that $U_0''(\bar{x}^*)$, up to a factor, equals the inverse of the integrated autocovariance in tree level approximation, because inverting this second derivative is trivial in Fourier domain (see Section IV D 1).

We would like to define an effective potential with the same properties as illustrated in this lowest order approximation, but valid beyond linear response approximation. To this end, we employ the MSR DJ formulation in what follows.

Relation between OM and MSR DJ effective actions As for the Onsager-Machlup form, we define the cumulant generating functional

$$W[j, \tilde{j}] = \ln \int \mathcal{D}x \int \mathcal{D}\tilde{x} \exp(S[x, \tilde{x}] + j^T x + \tilde{j}^T \tilde{x}). \quad (20)$$

To simplify notation, we will omit the index MSR DJ in the following main text if no confusion can occur.

Compared to its OM-form, $W[j, \tilde{j}]$ in addition incorporates the response properties of the system as differentiating once with respect to \tilde{j} and j each, respectively, yields the response function. The effective action in the MSRDJ formalism $\Gamma[x, \tilde{x}]$ is defined in analogy to (17) as the Legendre transform of $W[j, \tilde{j}]$

$$\Gamma[x^*, \tilde{x}^*] = \sup_{j, \tilde{j}} j^T x^* + \tilde{j}^T \tilde{x}^* - W[j, \tilde{j}]. \quad (21)$$

Like Z and W , Γ contains the full information of the system, including effects from noise-driven fluctuations. Approximating the integral in (20) over x and \tilde{x} by the maximum value of the integrand, that is by the path with maximal probability, leads to $\Gamma_0[x^*, \tilde{x}^*] = -S[x^*, \tilde{x}^*]$. Because this path ignores fluctuations, we also refer to it as the classical path or the saddle point approximation. Selecting only the stationary classical path, we obtain the minimum of U_0 .

The definition of Γ as the Legendre transform of W implies the important identities

$$\begin{aligned} \Gamma_x^{(1)}[x^*, \tilde{x}^*] &:= \frac{\delta}{\delta x} \Gamma[x^*, \tilde{x}^*] = j, \\ \Gamma_{\tilde{x}}^{(1)}[x^*, \tilde{x}^*] &:= \frac{\delta}{\delta \tilde{x}} \Gamma[x^*, \tilde{x}^*] = \tilde{j}, \end{aligned} \quad (22)$$

x^* and \tilde{x}^* are averages for given j, \tilde{j} and are implicitly given by the expressions (22), called equation of state, as extremal trajectories of Γ . Therefore, for the physical value $j = \tilde{j} = 0$ of the source fields, Γ plays the same role as the action for a classical particle, which motivates the notion of Γ as an effective action. In tree level approximation $\Gamma_0 = -S$, the set of equations (22) is then identical to (11) and (12). The implicit equations are self-consistent in x^* and \tilde{x}^* . To see this, we note that an analogous definition to (21) with $y = (x, \tilde{x})$ and $k = (j, \tilde{j})$ reads

$$\begin{aligned} \Gamma[y^*] &= -\ln \int_y \exp(S[y] + k^T(y - y^*)) \\ \text{with } \frac{\delta \Gamma}{\delta k} &\stackrel{!}{=} 0. \end{aligned} \quad (23)$$

The latter condition enforces that we integrate over ensembles of configurations that obey the constraint $\langle y \rangle = y^*$; in other words, the mean values for both fields x and \tilde{x} take the values given by the argument of Γ . The right hand side of (23) will hence depend via y^* on the approximation performed for Γ ; it takes on self-consistently determined values.

The information about the second cumulant of x is captured in the relation

$$\Gamma^{(2)} [x^*, \tilde{x}^*] = \begin{pmatrix} \frac{\delta^2 \Gamma[x^*, \tilde{x}^*]}{\delta x^2} & \frac{\delta^2 \Gamma[x^*, \tilde{x}^*]}{\delta x \delta \tilde{x}} \\ \frac{\delta^2 \Gamma[x^*, \tilde{x}^*]}{\delta \tilde{x} \delta x} & \frac{\delta^2 \Gamma[x^*, \tilde{x}^*]}{\delta \tilde{x}^2} \end{pmatrix} = \begin{pmatrix} \frac{\delta^2 W[j, \tilde{j}]}{\delta j^2} & \frac{\delta^2 W[j, \tilde{j}]}{\delta j \delta \tilde{j}} \\ \frac{\delta^2 W[j, \tilde{j}]}{\delta \tilde{j} \delta j} & \frac{\delta^2 W[j, \tilde{j}]}{\delta \tilde{j}^2} \end{pmatrix}^{-1} = [W^{(2)}]^{-1}, \quad (24)$$

that follows by differentiating (22). Differentiating the latter relation $n-1$ -times with respect to j , using $\frac{\partial}{\partial j} = \frac{\partial x^*}{\partial j} \frac{\partial}{\partial x^*} = (\Gamma^{(2)})^{-1} \frac{\partial}{\partial x^*}$, and repeated application of (24) yields expressions for the n -th cumulant, expressed in terms of derivatives of Γ [62, p. 115ff].

The use of the MSRDJ formalism simplifies the calculations of the effective action with respect to the Onsager-Machlup formalism. As a consequence of the response fields being only auxiliary variables, their expectation values vanish, i.e. $\langle \tilde{x}^n \rangle = 0 \ \forall n$ for solutions with stationary statistics (for a proof see Coolen [55] or appendix Section IV D). After exploiting the computational advantages of the MSRDJ formalism in the calculation Γ , it is convenient to obtain the Onsager-Machlup effective action, because it has a direct physical interpretation, where minima specify the mean and the curvature relates to fluctuations. We show in Section IV D that the two formulations are related by a Legendre transform

$$\Gamma_{\text{OM}}[x^*] = \sup_{\tilde{x}^*} \Gamma_{\text{MSRDJ}}[x^*, \tilde{x}^*]. \quad (25)$$

This specific choice of \tilde{x}^* conserves the full information on the fluctuations so that it is convenient to define the effective potential [36] as

$$U(\bar{x}^*) = \Gamma_{\text{OM}}[\bar{x}^*]/T. \quad (26)$$

Note, however, that the information on the response is lost as we have chosen \tilde{x} in dependence on x which, dually, fixes $\tilde{j} = 0$. Therefore, we cannot choose the perturbation \tilde{j} freely anymore. Eq. (25) holds for arbitrary statistics of the noise, while the analogous relation for the respective actions is in general not true if the noise is not Gaussian, as demonstrated by example in the appendix Section IV E, (59). The definition (25) hence makes the physically interpretable Onsager-Machlup effective action available even if an Onsager Machlup action S_{OM} cannot be formulated in the non-Gaussian case. Therefore, relating approximations of the respective effective actions can be nontrivial: Cooper et al. derived in [63] that Γ and Γ_{OM} of the KPZ-model yield the same effective equations if one performs a saddle-point approximation in the auxiliary fields of the Hubbard-Stratonovitch transform of the non-Gaussian parts of the respective actions. We here provide a general relation between the

two effective actions, that is valid in full generality beyond specific approximations. It may therefore be used to check whether a pair of approximations, each formulated for one of the two effective actions, is equivalent. The finding by Cooper et al. [63] is one such pair of equivalent approximations.

A simple special case arises if the noise, including all fluctuation corrections, remains Gaussian. The field \tilde{x} then still appears quadratically in the effective action. Taking the supremum over \tilde{x} in (25) is then identical to performing the integral over \tilde{x} . A corollary is that under these conditions, the Onsager-Machlup effective action has the same form as its tree level approximation (5), only with vertices $S^{(n)}$ replaced by effective vertices $-\Gamma^{(n)}$. For example the noise matrix $D = S_{\tilde{x}\tilde{x}}^{(2)}$ is replaced by $-\Gamma_{\tilde{x}\tilde{x}}^{(2)}$. We assume this special case in Figure 1 to determine the effective action including fluctuation corrections.

In summary, $U(\bar{x}^*)$ locally is the “energy landscape” that we are searching for and whose minimum is the true mean value in the stationary case taking into account all fluctuations. The curvature of $U(\bar{x})$ equals the inverse of the integrated covariance, as explained in Section IV D. The signature of a second order phase transition is hence the vanishing curvature of U at its minimum. A first order phase transition appears in systems where U has a flat segment. Note, however, that on a global scale, the identification of U with an energy landscape is not possible, because it assumes stationarity and is therefore only valid near a stable fixed point. As a consequence, the maxima of U do not indicate borders of the basin of attraction of this stable fixpoint, as it is expected for an energy. Moreover, unstable fixed points of the system will show up as minima, as is obvious in tree level approximation (18) that is positive semidefinite and vanishes whenever $f(x^*) = 0$. Thus we have found the local generalization of (19), where U_0 equals U in tree-level approximation.

B. Loop expansion

We have seen that the effective action provides an effective way to characterize the states of a stochastic system. We will now review a systematic expansion to compute Γ . Fluctuations provide corrections to the effective action that are commonly defined as Γ_{fl} by

$$\Gamma =: -S + \Gamma_{\text{fl}}.$$

In general it is not possible to compute Γ_{fl} exactly. Since Γ is convex by construction, it is convenient to expand it about its minimum, which, according to (22), defines the true mean value of x . This minimum is unique in systems away from first order phase transitions. This is a standard approach in statistical physics and quantum field theory where it is known as the loop expansion. For an introduction, consult for example the books by Kleinert [48, chap. 3.23.] or Zinn-Justin [4, , chap. 7.7.ff]. This technique has first been applied in the context of neuronal networks by Buice and Chow [64], recently reviewed in [7, 8].

Despite these excellent reviews, we here briefly outline the loop expansion on the concrete example for four reasons. First, all terms in the action are at least of linear order in the response field \tilde{x} ; its equation of state therefore always admits a trivial solution $\tilde{x} \equiv 0$ and the $\tilde{x}\tilde{x}$ -propagator vanishes. These are features specific to the MSRDJ formalism that deserve some comments. Second, to introduce the diagrammatic notation, because the diagrams that appear in the less standard functional renormalization group method derive from those of the loop expansion. Third, the loop expansion gives us the leading order fluctuation corrections beyond tree level. They therefore show us which new vertices will be generated along the renormalization group flow. And forth, because the loop expansion provides a systematic way to derive self-consistency equations for the mean of a process, an idea that is conceptually continued in the functional renormalization group approach.

In contrast to mean field theory, the loopwise expansion can be improved systematically because it is an expansion in a parameter that measures the fluctuation strength, often related to the system size. Here, we consider a one-dimensional system, but it also depends on a small parameter that organizes the loop expansion, as we will demonstrate below.

To lowest order we simply neglect all fluctuations which means $\Gamma_{\text{fl}} = 0$ and therefore $\Gamma = -S$. This is called the tree-level or mean-field approximation (see discussion of the classical path above). Corrections to this approximation are typically expressed by Feynman diagrams (sometimes referred to as Mayer graphs [59, 65]) whose constituents are determined by the underlying theory. We deliberately switch between the representation of the diagrammatic elements in time or frequency space depending on the form of the problem. In theories in which the quadratic part of the action constitutes a solvable theory, as is the case here, expansions in the non-quadratic part of the action involve expectation values of terms quadratic in x and \tilde{x} . We call

$$\Delta(t-s) = \begin{pmatrix} \langle x(t)x(s) \rangle & \langle x(t)\tilde{x}(s) \rangle \\ \langle \tilde{x}(t)x(s) \rangle & \langle \tilde{x}(t)\tilde{x}(s) \rangle \end{pmatrix} = \begin{pmatrix} x(t) \xleftarrow{x(s)} x(t) \xleftarrow{\tilde{x}(s)} & \\ \tilde{x}(t) \xrightarrow{x(s)} & 0 \end{pmatrix}$$

the propagators of the theory. Further ingredients are the interaction vertices which, in general, are given by the non-quadratic components of the action, in our case the Fourier coefficients of the term $\tilde{x}f(x)$.

Henceforth, we consider the corrections to the mean value, the variance and one of the three-point vertices in the neuroscientific case, where $f(x) = -x + Jg(x)$. For small activities we can expand the gain function and keep only its linear and quadratic terms. This is in line with the observation that activation functions are typically convex in the vicinity of the working point [66]. We define

$$g(x) = x + \alpha x^2.$$

Therefore, the only bare vertex (i.e. the only vertex that is also present in the action) is $S_{\tilde{x}xx}^{(3)}$. We choose this quadratic nonlinearity also for pedagogical reasons, as it constitutes the simplest nontrivial example which is suitable to demonstrate the methods that we will develop. For practical calculations it is convenient to switch the parameterization to

$$f(x) = -lx + \beta x^2, \quad (27)$$

where $l = 1 - J > 0$ and $\beta = \alpha J > 0$. Then in frequency domain the bare propagator reads

$$\begin{aligned} \Delta^0(\omega, \omega') &= (-S^{(2)})^{-1} = \left(\begin{pmatrix} 0 & -i\omega + m \\ i\omega + m & -D \end{pmatrix} \frac{\delta(\omega + \omega')}{2\pi} \right)^{-1} \\ &= \begin{pmatrix} \frac{D}{\omega^2 + m^2} & \frac{1}{-i\omega + m} \\ \frac{1}{i\omega + m} & 0 \end{pmatrix} 2\pi \delta(\omega + \omega'), \end{aligned} \quad (28)$$

where $m = -l + 2\beta x^*$ plays the role of a mass-like term in the theory. For the definition of the Fourier transform, as we use it throughout this text, see [Section IV L](#). Similarly, for the interaction vertex we obtain

$$\begin{array}{c} X(\omega_2) \\ \swarrow \\ \bullet \\ \nwarrow \\ X(\omega_1) \end{array} \begin{array}{c} \tilde{X}(\omega_3) \\ \rightarrow \end{array} = \frac{1}{2} S_{\tilde{X}XX}^{(3)} = -\frac{\beta}{(2\pi)^2} \delta(\omega_1 + \omega_2 + \omega_3).$$

We notice that the frequencies are conserved at each vertex and each propagator. Since in the action $S[x, \tilde{x}]$ the function $f(x)$ is multiplied with one \tilde{x} , see (15), we conclude that

two interaction vertices and two amputated legs, also called self-energy corrections,

$$\Gamma_{\tilde{X}X,\text{fl.}}^{(2)}(\sigma_1, \sigma_2) = (-1) \begin{array}{c} \sigma_1 \\ \curvearrowright \\ \text{---} \\ \curvearrowleft \\ \sigma_2 \end{array} = \left[\Gamma_{X\tilde{X},\text{fl.}}^{(2)}(\sigma_1, \sigma_2) \right]^*$$

$$\Gamma_{\tilde{X}\tilde{X},\text{fl.}}^{(2)}(\sigma_1, \sigma_2) = -\frac{1}{2} \begin{array}{c} \sigma_1 \\ \curvearrowright \\ \text{---} \\ \curvearrowleft \\ \sigma_2 \end{array},$$

which evaluate to

$$\Gamma_{\text{fl.}}^{(2)}(\sigma_1, \sigma_2) = \begin{pmatrix} 0 & \frac{1}{-i\sigma_1+2m} \\ \frac{1}{i\sigma_1+2m} & \frac{D}{\sigma_1^2+(2m)^2} \end{pmatrix} \frac{2\beta^2 D}{2\pi m} \delta(\sigma_1 + \sigma_2).$$

Making use of the property of the Legendre transform (24), we obtain the one-loop approximation of the propagator and hence, the variance and the response functions, see [Section IV G](#).

Finally, we consider the three-point interaction vertex.

$$\Gamma_{\tilde{X}XX,\text{fl.}}^{(3)}(\sigma_1, \sigma_2, \sigma_3) = -8 \left[\begin{array}{c} \sigma_2 \quad \sigma_3 \\ \curvearrowright \quad \curvearrowright \\ \text{---} \\ \curvearrowleft \quad \curvearrowleft \\ \sigma_1 \end{array} + \sigma_2 \leftrightarrow \sigma_3 + \begin{array}{c} \sigma_2 \quad \sigma_3 \\ \curvearrowright \quad \curvearrowright \\ \text{---} \\ \curvearrowleft \quad \curvearrowleft \\ \sigma_1 \end{array} \right]$$

$$= -\frac{8\beta^3 D}{(2\pi)^2 m (2m + i\sigma_1) (2m - i\sigma_2) (2m - i\sigma_3)} \delta(\sigma_1 + \sigma_2 + \sigma_3).$$

For the corresponding expression in time domain, see [Section IV H](#).

A comparison between the fluctuation corrections $\Gamma_{\text{fl.}}$ and the corresponding terms in the action S reveals that $\Gamma_{x\tilde{x},\text{fl.}}^{(2)}$ counteracts the tree-level contribution m , whereas the $\tilde{x}\tilde{x}$ - and the $\tilde{x}xx$ -contributions are enhanced. Therefore, the linear term m of the differential equation gets weakened such that for large noise it could even effectively vanish. This would correspond to a second order phase transition signalled by the divergence of fluctuations. However, we are unable to explore this regime due to fundamental constraints inherent to our setting that we will discuss at the end of this section. Due to conservation of frequencies at the vertex, there are only corrections for the zero frequency mode of the mean value (panel A in [Figure 2](#)). Also the corrections to the propagator (panel C, D in [Figure 2](#))

and the three-point vertex are largest for $\sigma_i = 0$ and decay algebraically with increasing frequency. Figure 2, A and B show the mean value and the variance for varying strength of the nonlinearity β and different methods, where we use the solution by the Fokker-Planck equation [58] as the ground truth, which indeed agrees very well with the simulated results. In particular, we observe that the one-loop-approximation is markedly better than the tree-level approximation, which predicts $\langle x \rangle = 0$ and $\langle\langle x^2 \rangle\rangle = 0.17$ for all β . The same holds true for the xx -part of the propagator, which is the power spectrum of the process, as shown in Figure 2, panel C. The fluctuation corrections here in particular lead to an elevation of the power at low frequencies. This qualitative effect only depends on coarse features of the system, such as the convexity of the non-linearity. One may therefore expect qualitatively similar features in networks which operate in regimes in which the neuronal transfer function is expansive, as typical for the low rate regimes of the cortex [66].

In principle we could try to find a more accurate approximation of the effective action by going to higher loop orders. However, this already becomes unwieldy at the next order because the number of diagrams increases quickly and the integration of the loop momenta becomes numerically expensive. Instead, we will below use renormalization group techniques to obtain self-consistency at arbitrary levels of the statistics.

Even though the one-loop calculations are not confined to a certain parameter range, we may not disregard the fact that strictly speaking there is no stationary solution for our particular choice for $g(x)$, because x escapes towards infinity almost surely for $t \rightarrow \infty$. However, for finite times and $l/\beta \gg \sqrt{D}$, the second unstable fixed point $x_1 = l/\beta$ is far away from the stable fixed point $x_0 = 0$ measured in units of the fluctuations. Therefore, the escape probability is negligible and we confine our analysis to this case by effectively setting the escape probability to zero; in particular for the otherwise exact Fokker-Planck solution to which we compare the results of the loop expansion. A rigorous analysis of this setting is a problem on its own requiring the introduction of a probability for a path conditioned on the requirement that it has not escaped to infinity. For a leak term equal to zero, this analysis has recently been performed [67]. Another possibility is to consider the time-dependent problem, as it is done for example in the context of laser physics [68]. Obviously, we increase the escape probability by decreasing the leak term, which amounts to approaching the critical point. These two effects cannot be decoupled by appropriately redefining the noise level D . We see this by rescaling the time as $s = lt$ and accordingly the

fields $\tilde{y}(s) = \sqrt{D/l} \tilde{x}(t)$ and $y(s) = \sqrt{l/D} x(t)$ which leads to

$$S[\tilde{y}, y] = \int ds \left[\tilde{y}^T (\partial_s + 1) y - \beta' \tilde{y}^T y^2 + \tilde{y}^T \frac{1}{2} \tilde{y} \right], \quad \text{where } \beta' = \sqrt{\frac{D}{l^3}}.$$

The unstable fixed point is then given by $x_0 = 1/\beta'$ in the noise-less case. Therefore, β' is the only free parameter of the model and the strength of the nonlinearity determines also the distance between the stable and the unstable fixed point. So it is impossible to find a set of parameters where the system operates far from the unstable fixed point so that the expansion around the stable fixed point is accurate and where concurrently the effect of the nonlinearity is stronger than the linear part.

In the next chapter, we will demonstrate by comparing to simulations that neglecting the possibility of escaping is justified in the presence of a leak term for sufficiently low noise and nonlinearity.

C. Time dependence of statistics

The effective potential contains information about the stationary time-averaged statistics of the system; in particular the mean value and the variance at vanishing frequency. But applications often also require us to study the time-dependent response of the system. In the context of neuronal networks, for example, we would like to quantify the response of the system to an applied stimulus. The simplest approximation (3) that neglects the effect of the noise also provides us with the lowest order approximation of such a response. In the following we will see how the effective action (21) allows us to systematically improve this approximation by deriving an effective differential equation for the mean value. We have to treat \tilde{x} (dually: \tilde{j}) as an independent variable because we want to study the effect that the past trajectory $x(t)$ has on its future. From another perspective, this is equivalent to studying the response of $x(t)$ to a certain perturbation, namely to its own past. This view will also provide direct interpretations for the vertex functions: they appear as convolution kernels in the effective equation of motion for the moments of the system.

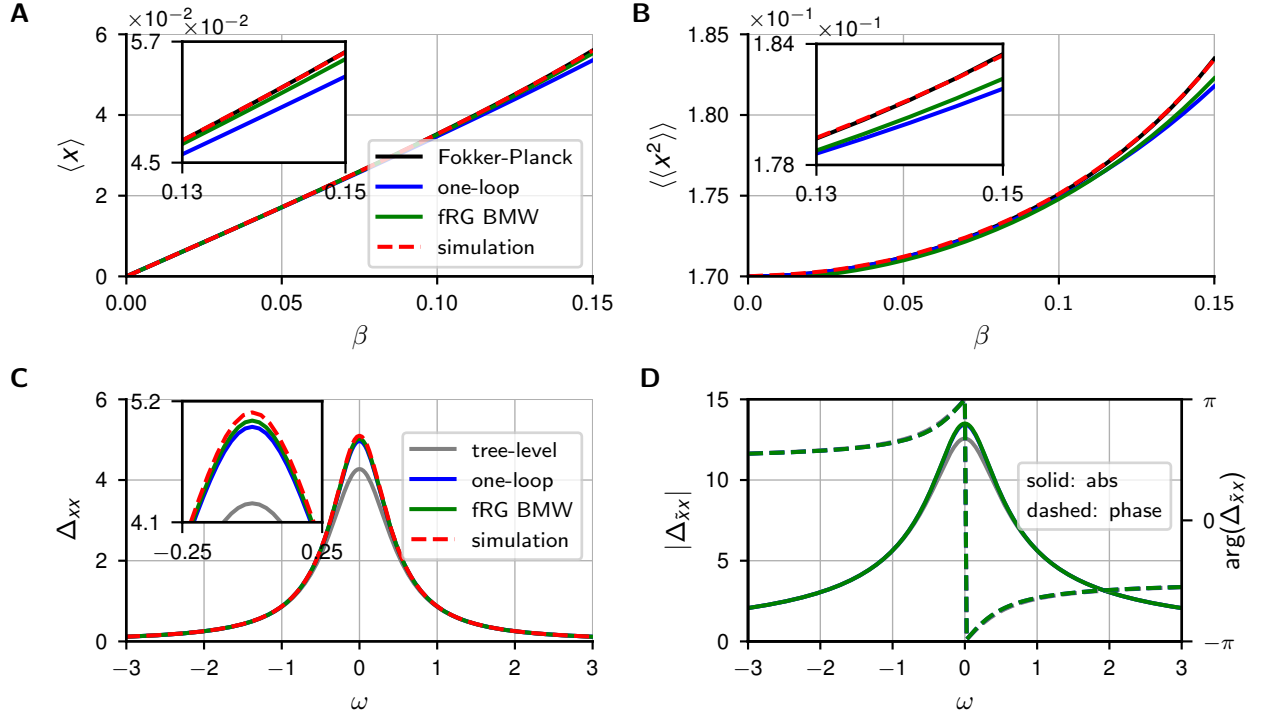


Figure 2. Mean (A) and variance (B) as functions of the strength β of the nonlinearity for different methods. Parameters: $l = 0.5$, $D = 0.17$. (C) Power spectrum of the system from simulations compared to different approximations. (D) Absolute value (solid lines) and phase (dashed lines) of the response function. The results of the one-loop and the fRG BMW approximation coincide at this resolution. For comparison between simulations and theory results of the response of the system was subject to small (but not infinitesimally small) perturbations, see Section II C, Figure 3. Parameters for (C) and (D): $l = 0.5$, $D = 0.17$ and $\beta = 0.15$.

Effective equations of motion

It turns out that it is convenient to expand Γ around a reference point $(\bar{x}, \bar{\tilde{x}})$

$$\begin{aligned}
 \Gamma[x^*, \tilde{x}^*] &= \sum_{n=0}^{\infty} \sum_{m=0}^{\infty} \frac{1}{n!m!} \frac{\delta^{n+m}\Gamma}{(\delta x^*)^n (\delta \tilde{x}^*)^m} [\bar{x}, \bar{\tilde{x}}] \delta x^n \delta \tilde{x}^m \\
 &= \text{const.} + \Gamma^{(1)}[\bar{x}, \bar{\tilde{x}}] \begin{pmatrix} \delta x \\ \delta \tilde{x} \end{pmatrix} + \frac{1}{2} \begin{pmatrix} \delta x \\ \delta \tilde{x} \end{pmatrix}^T \Gamma^{(2)}[\bar{x}, \bar{\tilde{x}}] \begin{pmatrix} \delta x \\ \delta \tilde{x} \end{pmatrix} + \dots,
 \end{aligned} \tag{30}$$

where we introduced the derivatives $\frac{\delta^{n+m}\Gamma}{(\delta x^*)^n (\delta \tilde{x}^*)^m}$ as covectors, the deflections $\delta x(t) := x^*(t) - \bar{x}$ and $\delta \tilde{x}(t) := \tilde{x}^*(t) - \bar{\tilde{x}}$ together with the notation

$$\begin{aligned} & \frac{\delta^{n+m}\Gamma}{(\delta x^*)^n (\delta \tilde{x}^*)^m} [\bar{x}, \bar{\tilde{x}}] \delta x^n \delta \tilde{x}^m \\ := & \prod_{i=1}^n \int dt_i \prod_{j=1}^m \int ds_j \left. \frac{\delta^{n+m}\Gamma [x^*, \tilde{x}^*]}{\delta x^*(t_1) \dots \delta x^*(t_n) \delta \tilde{x}^*(s_1) \dots \delta \tilde{x}^*(s_m)} \right|_{x^*=\bar{x}, \tilde{x}^*=\bar{\tilde{x}}} \delta x(t_1) \dots \delta x(t_n) \delta \tilde{x}(s_1) \dots \delta \tilde{x}(s_m) \end{aligned} \quad (31)$$

$$=: \Gamma \begin{matrix} (n+m) \\ \underbrace{x \dots x}_{n\text{-times}} \quad \underbrace{\tilde{x} \dots \tilde{x}}_{m\text{-times}} \\ \delta x^n \delta \tilde{x}^m \end{matrix}.$$

We determine the true mean values \bar{x} and $\bar{\tilde{x}}$ of the two fields by solving the two implicit equations $\Gamma^{(1)} [x^*, \tilde{x}^*] \stackrel{!}{=} 0$ (compare (22)). All further Taylor coefficients (or Volterra kernels) in (30) have physical meanings. $\Gamma_{\tilde{x}\tilde{x}}^{(2)}$ includes all corrections to the Gaussian component of the noise and the mixed derivatives represent the renormalized response functions. Consequently, $\Gamma^{(2)}$ contains the corrections to the second cumulant since it is the inverse of $W^{(2)}$. The Taylor coefficients of order n describe the interdependence of measurements at n points in time. We make this more explicit by considering $\Gamma_{\tilde{x}x}^{(3)}$ in the equation of state $\frac{\delta}{\delta \tilde{x}^*(t)} \Gamma [x^*, \tilde{x}^*] = 0$, which, using the decomposition $\Gamma = -S + \Gamma_{\text{fl}}$, takes the form

$$\begin{aligned} 0 = & - \left(\frac{\partial}{\partial t} - f'(\bar{x}) \right) \delta x(t) - D \delta \tilde{x}(t) + \frac{1}{2} f''(\bar{x}) \delta x(t) \delta x(t) + \dots \\ & + \int ds \Gamma_{\tilde{x}x, \text{fl}}^{(2)}(t, s) \delta x(s) + \int ds \Gamma_{\tilde{x}\tilde{x}, \text{fl}}^{(2)}(t, s) \delta \tilde{x}(s) \\ & + \frac{1}{2} \int ds \int du \Gamma_{\tilde{x}xx, \text{fl}}^{(3)}(t, s, u) \delta x(s) \delta x(u) + \dots, \end{aligned} \quad (32)$$

$$\begin{aligned} 0 = & \left(-\frac{\partial}{\partial t} - f'(\bar{x}) \right) \delta \tilde{x}(t) - f''(\bar{x}) \delta \tilde{x}(t) \delta x(t) + \dots \\ & - \int ds \Gamma_{\tilde{x}x, \text{fl}}^{(2)}(s, t) \delta \tilde{x}(s) \\ & - \int ds \int du \Gamma_{\tilde{x}xx, \text{fl}}^{(3)}(s, t, u) \delta \tilde{x}(s) \delta x(u) + \dots \end{aligned} \quad (33)$$

Thus, Γ_{fl} accounts for the corrections due to the noise. Additionally, we neglect all higher order terms as well as the remaining components of $\Gamma^{(3)}$, which are subleading as we discuss in Section IID after (44). Looking at the fluctuation corrections in (32) and (33), we notice that in general the noisy system exhibits interactions that are non-local in time (cf. (31)) even if the deterministic system does not contain such terms. As a consequence, it is not possible to define a potential for which $\partial_t x(t) = -\partial_x V(x)$ even if we set $\tilde{x} = 0$, in

contrast to the tree-level approximation of a one-dimensional system. The first occurrence of an effective equation of motion as (32) and (33) in the context of neuronal networks has been presented in [69, eqs. (42) and (43)] using the Doi-Peliti formalism [70, 71] applied to Markovian systems with discrete state spaces.

Why is time-dependence captured by vertex functions?

In the previous chapter we searched only for (quasi) stationary solutions of the quantities that describe the system. Still, (32) and (33) are two coupled integro-differential equations, so obviously describing quantities that evolve in time. At a first glance, this might occur contradictory. However, this is not so, as we see by the following consideration: After discretizing time by t_0, t_1, \dots, t_{N-1} , all functionals calculated above are just functions of an N -dimensional vector $\mathbf{x} := (x_0, \dots, x_{N-1}) := (x(t_0), \dots, x(t_{N-1}))$. Finding stationary solutions then corresponds to knowing the respective quantities on the line $\bar{\mathbf{x}} = \bar{x} \cdot (1, 1, \dots, 1)$, $\bar{x} \in \mathbb{R}$. Nevertheless, if Γ is an analytic function of \mathbf{x} and we know all partial derivatives $\Gamma^{(n)}$ with respect to $x_i, 0 \leq i < N$ evaluated at $\bar{\mathbf{x}}$, we know Γ for arbitrary vectors \mathbf{x} . Along the same lines, knowing only the first few derivatives gives us an approximation for small but arbitrarily directed perturbations around $\bar{\mathbf{x}}$. Therefore, drawing the continuum limit, we conclude that knowing functional derivatives evaluated at stationary $x(t) = \bar{x}$ up to a certain order allows us to study small perturbations with arbitrary time dependence around \bar{x} .

Relaxation of a small departure from the mean

As an example, we consider the deflection of the system from its mean value at time $t_0 = 0$ and examine the equation of motion that describes its relaxation back to the baseline. We ensure that we consider only non-escaping trajectories by setting $\tilde{x} \equiv 0$ (see Section IV B). By inserting the tree-level approximation $\Gamma_{\text{fl.}} = 0$ into (32), we obtain

$$\partial_t \delta x(t) = -l \delta x(t) + \beta \delta x(t)^2,$$

which we can integrate analytically

$$\delta x(t) = \frac{l}{\beta} \frac{1}{1 + e^{lt} \left(\frac{l}{\beta c} - 1 \right)} = c e^{-(l-c\beta)t + \mathcal{O}((lt)^2)} + \mathcal{O}\left(\left(\frac{\beta c}{l}\right)^2\right), \text{ where } c = \delta x(0).$$

We notice that the second term in the denominator is due to the nonlinearity and leads to a slower relaxation of the system back to its mean value compared to the time constant l^{-1}

of the linear part of the dynamics. In one-loop approximation, the equation of motion reads

$$\begin{aligned}
\partial_t \delta x(t) = & m \delta x(t) + \beta \delta x(t)^2 \\
& - \frac{2\beta^2 D}{m} \int_{t_0}^t dt' \underbrace{e^{2m(t-t')}}_{\propto \Gamma_{\tilde{x},\text{fl.}}^{(2)}(t,t')} \delta x(t') \\
& - \frac{8\beta^3 D}{m} \int_{t_0}^t dt' \int_{t_0}^t dt'' \underbrace{H(t'-t'') e^{2m(t-t'')}}_{\propto \Gamma_{\tilde{x}x,\text{fl.}}^{(3)}(t,t',t'')} \delta x(t') \delta x(t''). \tag{34}
\end{aligned}$$

Let us inspect the single terms in (34) in more detail: The first line is the tree-level contribution. $\Gamma_{\text{fl.}}^{(2)}$ mediates a linear self-feedback for the departure δx of the process from its stationary value. One of the interpretations of $\Gamma_{\tilde{x}x}^{(3)}$, writing it as $\Gamma_{\tilde{x}x}^{(3)}(t, t', t'') = \frac{\delta}{\delta x(t'')} \Gamma_{\tilde{x}x}^{(2)}(t, t')$, is that it quantifies the change of the linear response kernel of the self-energy at times t, t' due to a change of the activity at time t'' . In conclusion, only the interplay between an interaction and noise, as apparent by the prefactors composed of both β and D , creates memory in the system and hence the effective equation of motion for departures of the mean become non-local in time. This phenomenon is generally observed if certain degrees of freedom (in our case the variance) are implicitly taken into account to describe the quantity of interest [72, e.g. chap. 1.6].

The correction to the linear term has the opposite sign compared to the term stemming from the bare interaction. Furthermore, the three-point interaction gets enhanced by the fluctuation corrections, so that in total, the relaxation is slower than in the deterministic system. An alternative way to arrive at (34) is to derive ODEs for the first two moments from the Fokker-Planck equation [58] and to use a Gaussian closure. Details are shown in Section IV I, where we also demonstrate that the loop expansion (34) amounts to a Taylor expansion of the Fokker-Planck solution in δx . Figure 3 compares this approximation to the one-loop result. Indeed, the semi-logarithmic plot of the relaxation as a function of time shows an elevated time constant due to fluctuations compared to the tree-level approximation. Analyzing the origin of the elevated time constant, Figure 3C compares the different contributions to the right hand side of (34). The linear part of the tree-level approximation yields the largest contribution. For sufficiently long times, we find that the linear part of the one-loop correction comes next. This shows that only the cooperation of the non-linearity with the fluctuations in the system cause this correction and are more important than the non-linearity itself, the quadratic tree level contribution. Interplay of

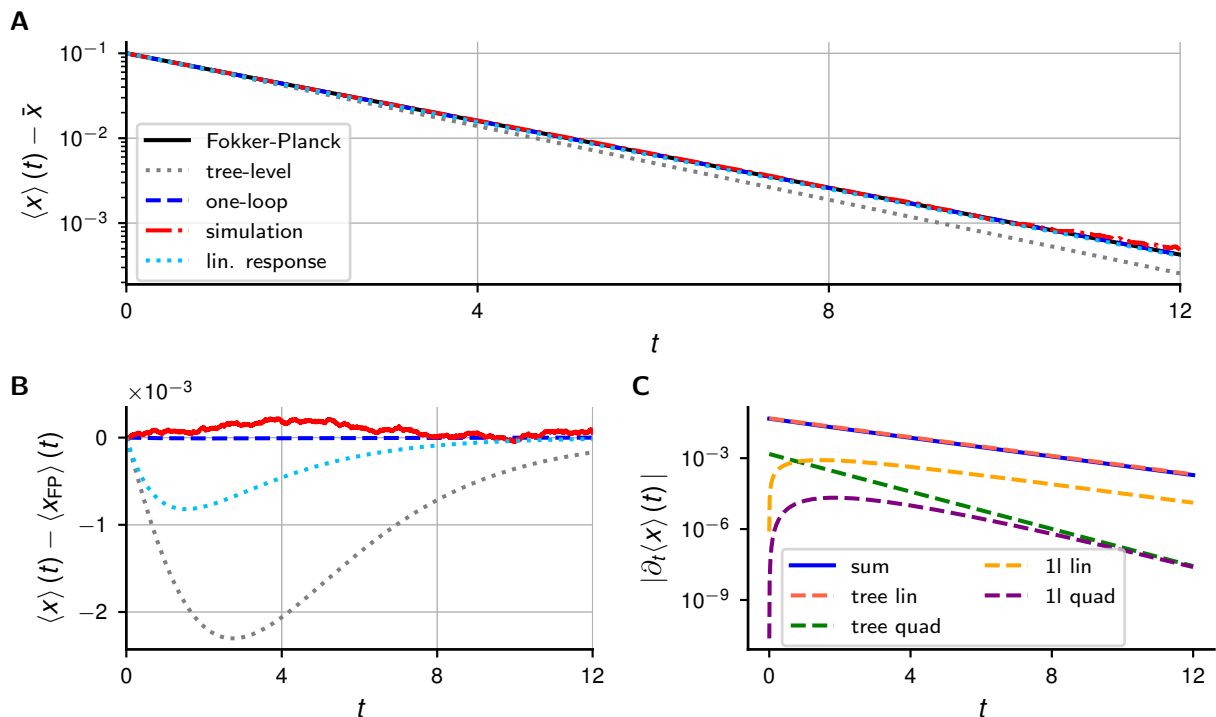


Figure 3. Relaxation after deflection described by effective equation of motion. The one-loop result is given by (34) and the Fokker-Planck result by the coupled differential equations (62) and (63). For the simulations, the system is thermalized and then deflected by adding a small perturbation δx_0 to the current value of x after which it relaxes back to its stationary state. (A) shows the average over $2.9 \cdot 10^9$ trials of the relaxation process and (B) the difference between the various approximations and the simulation to the Fokker-Planck result. The linear response (dotted light blue) contains solely the terms in (34) that are linear in δx . (C) Different contributions to the right hand side of (34). Sum shows the full right hand side (blue); linear part in δx of the tree level term (dashed salmon pink); quadratic part in δx of the tree level terms (dashed green); linear term of one-loop correction (dashed yellow); quadratic term of one-loop corrections (dashed violet).

noise and nonlinearities hence causes a longer memory in the system's response.

Power spectrum So far we have discussed an effective equation of motion for the mean value of the process that also allowed us to obtain an interpretation for the various vertex functions. We can ask a corresponding question for the second order statistics, namely whether there is a linear system that possesses the same second order statistics as the full non-linear system. Such a reduction may be useful to obtain insights into the structure of

network fluctuations and also to reduce the complexity of stochastic non-linear systems to simpler, linear ones.

Indeed, we can use the expressions for the derivatives of the effective action to write down the action of a linear system that, up to second order, reproduces the stationary statistics of the full system. To this end we define

$$S_{\text{lin}} := - \left(\delta \tilde{x}^T \Gamma_{\tilde{x}x}^{(2)} \delta x + \frac{1}{2} \delta \tilde{x}^T \Gamma_{\tilde{x}\tilde{x}}^{(2)} \delta \tilde{x} \right). \quad (35)$$

The corresponding equation of motion reads

$$\frac{d}{dt} \delta x(t) = -l \delta x(t) + \int dt' \Gamma_{\tilde{x}x,\text{fl.}}^{(2)}(t, t') \delta x(t') + \xi(t), \quad (36)$$

$$\text{where } \langle \xi(t) \rangle = 0 \text{ and } \langle \langle \xi(t) \xi(t') \rangle \rangle = D \delta(t - t') + \Gamma_{\tilde{x}\tilde{x},\text{fl.}}^{(2)}(t, t').$$

By construction this stochastic integro-differential equation (36) reproduces the stationary variance $\Delta_{xx}(t, s) = W_{xx}^{(2)}(t, s) = \langle \delta x(t) \delta x(s) \rangle$ as well as the linear response $\Delta_{x\tilde{x}}(t, s) = W_{x\tilde{x}}^{(2)}(t, s) = \langle \delta x(t) \delta \tilde{x}(s) \rangle$ of the full system, because the solution of the Gaussian system (35) implicitly inverts the kernel $\Gamma^{(2)}$, which, by (24), yields the covariance matrix $W^{(2)}$. We could also take into account the effect of transient values of $x(t)$ on the variance to obtain a corresponding reduction that is valid in the non-stationary case. For this, however, we would need to know $\Gamma_{\tilde{x}x,\text{fl.}}^{(2)}$ evaluated at arbitrary $x(t)$. In this case, it is therefore more convenient to use the second Legendre transform that treats the variance as given, just like x^* in the case of the first Legendre transform, as shown by Bravi and co-workers [73].

The construction of a linear system leads to a new perspective of the effect of the nonlinearity: Up to the second cumulant the nonlinear system is equivalent to a linear one with a specific causal memory kernel and a corresponding non-white Gaussian noise term, caused by the self-energy correction $\Gamma_{\tilde{x}\tilde{x}}^{(2)}$.

D. Functional Renormalization Group

The loopwise expansion, by virtue of approximating the effective action, yields self-consistent equations for the mean. But we saw above that also the second order statistics and the higher order vertex functions experience fluctuation corrections. One would therefore like to have a scheme that is self-consistent also with regard to these higher order vertex functions.

One possible approach that has led to reasonable results, is to correct the mean, the propagator and the interaction vertex by the one-loop results and therein replace the bare quantities by the corrected ones to gain an even better approximation. This procedure is repeated until the result eventually converges. This approach corresponds to taking into account only specific diagrams with infinitely many loops and is called self-consistent one-loop approximation. It typically corrects the mean value and the self-energy while keeping the interaction vertices at their bare values; it is then known as the “Hartree-Fock approximation” [8, 59]. But of course this scheme can be extended to arbitrary order of the vertex functions. A formal way to derive such approximations systematically is by multiple Legendre transforms, an idea going back to the seminal work by De Dominicis and Martin [74]: One re-expresses interaction potentials in terms of connected correlation functions. Parquet equations are, for example, obtained by the fourth Legendre transform of an even theory [see e.g. 59, for a review, especially chap. 6.2.10].

We here want to follow a different scheme that is inherently self-consistent to arbitrary desired orders, the functional renormalization group (fRG). The fRG scheme naturally takes into account fluctuation corrections by renormalizing the mean value, the propagators, and all interaction vertices simultaneously.

Technically, the functional Renormalization Group (fRG) [35] is an alternative way to calculate Γ . It is one of the exact Renormalization Group (eRG) schemes [36, 75, 76], in essence going back to the seminal work by Wegner and Houghton [34]. It does not rely on an expansion in a small parameter, in contrast to the loopwise expansion, but it is nevertheless represented by diagrams with a one-loop structure. The technique induces an infinite hierarchy of coupled differential equations for $\Gamma^{(n)}$, so that in practice, we have to apply approximations, typically by truncating the hierarchy. Yet, this technique is, as all eRG-schemes, exact only on the level of the full functional $\Gamma[x, \tilde{x}]$ and not for a particular truncation in terms of a subset of $\Gamma^{(n)}$. However, fRG provides a framework to effectively construct approximations in a similar spirit as the self-consistent one-loop approximation and its systematic extensions.

The essential technical trick of the fRG is to simplify the theory by adding an initially large quadratic term, the regulator R_λ , to the action. It is a differentiable function of a so

called flow parameter λ and can be chosen arbitrarily up to the following properties:

$$\lim_{\lambda \rightarrow \Lambda} |R_\lambda| = \infty \text{ and } \lim_{\lambda \searrow 0} R_\lambda = 0. \quad (37)$$

The first property ensures that the theory for $\lambda = \Lambda$ has no fluctuations and its vertices correspond to the ones of the bare action, while for $\lambda = 0$, the original system is recovered. To arrive at this case and interpolate between both limits, an ODE for the effective action is derived by differentiating with respect to λ . This is the Wetterich equation [35], whose derivation for our setting, in particular for the presence of the response field, we will sketch in the following adhering to the conventions of Berges et al. [36].

Since the regulator R_λ is intended to suppress fluctuations, it is sufficient for our case to add it to the off-diagonal terms of the free part of the action: by (28) it will hence appear at the same position as the leak term m , thus controlling the variance of the fluctuations. We thus define

$$\begin{aligned} S_\lambda [X, \tilde{X}] &= S_0 [X, \tilde{X}] + \Delta S_\lambda [X, \tilde{X}] + S_{\text{int}} [X, \tilde{X}], \quad \text{where} \\ \Delta S_\lambda [X, \tilde{X}] &= -\frac{1}{2} \int \frac{d\omega}{2\pi} \begin{pmatrix} X(-\omega) \\ \tilde{X}(-\omega) \end{pmatrix} \frac{1}{2} R_\lambda \sigma_x \begin{pmatrix} X(\omega) \\ \tilde{X}(\omega) \end{pmatrix} \\ S_{\text{int}} [X, \tilde{X}] &= -\beta \int \frac{d\omega}{2\pi} \int \frac{d\omega'}{2\pi} \tilde{X}(\omega) X(\omega') X(-\omega - \omega'), \end{aligned} \quad (38)$$

where $\sigma_x = \begin{pmatrix} 0 & 1 \\ 1 & 0 \end{pmatrix}$ denotes the first Pauli matrix. Therefore, the bare propagator reads

$$\Delta_\lambda^0(\omega, \omega') = \begin{pmatrix} \frac{D}{\omega^2 + (m + \frac{1}{2}R_\lambda)^2} & \frac{1}{-i\omega + m + \frac{1}{2}R_\lambda} \\ \frac{1}{i\omega + m + \frac{1}{2}R_\lambda} & 0 \end{pmatrix} 2\pi \delta(\omega + \omega').$$

We notice that R_λ has to be negative to avoid a vanishing leak term (since $m < 0$) and thus a fluctuation singularity at $\omega = 0$ along the trajectory. We define $\tilde{\Gamma}_\lambda [X^*, \tilde{X}^*]$ as the Legendre transform of the cumulant generating functional, given by

$$W_\lambda [J, \tilde{J}] = \ln \int \mathcal{D}X \int \mathcal{D}\tilde{X} \exp(S_\lambda [X, \tilde{X}] + J^T X + \tilde{J}^T \tilde{X}),$$

where we used the abbreviation $J^T X = \int d\omega J(\omega) X(\omega)$. Defining Γ_λ , we remove the “direct” effect of the regulator

$$\Gamma_\lambda [X^*, \tilde{X}^*] := \tilde{\Gamma}_\lambda [X^*, \tilde{X}^*] + \Delta S_\lambda [X^*, \tilde{X}^*],$$

so that $\lim_{\lambda \rightarrow \Lambda} \Gamma_\lambda = -S$ and $\lim_{\lambda \rightarrow 0} \Gamma_\lambda = \Gamma$. To derive the flow equation for the effective action of the theory defined in (38), we take the partial derivative of W_λ with respect to the flow parameter and deduce from this the respective derivatives of $\tilde{\Gamma}_\lambda$ and Γ_λ (for details consult appendix Section IV J), which results in the Wetterich equation

$$\begin{aligned} \frac{\partial \Gamma_\lambda [X^*, \tilde{X}^*]}{\partial \lambda} &= \frac{1}{2} \text{Tr} \left\{ \Delta_{\tilde{X}X, \lambda} \frac{\partial R_\lambda}{\partial \lambda} \right\} \\ &= \frac{1}{2} \text{Tr} \left\{ \left[\Gamma_\lambda^{(2)} [X^*, \tilde{X}^*] + \frac{1}{2} R_\lambda \sigma_x \right]_{\tilde{X}X}^{-1} \frac{\partial R_\lambda}{\partial \lambda} \right\} = \frac{1}{2} \text{Tr} \left(\text{circle with square} \right), \end{aligned} \quad (39)$$

where in this section, lines denote full propagators

$$\Delta_\lambda := \left(\tilde{\Gamma}_\lambda^{(2)} \right)^{-1} = \left(\Gamma_\lambda^{(2)} + \frac{1}{2} R_\lambda \sigma_x \right)^{-1} \quad (40)$$

and open squares represent $\frac{\partial R_\lambda}{\partial \lambda}$. For the final result ($\lambda = 0$), the choice of the concrete form of R_λ is arbitrary as long as it fulfills (37) and does not lead to acausal in the action. The interpretation of Γ_λ along the trajectory of the flow equations, however, depends on the regulator.

The simplest choice is the uniform regulator, for example $R_\lambda = -\lambda$. In this case all frequencies get damped equally. Its equivalence to an additional leak term (compare (15) and (40)) bears a second interpretation: We may as well interpret each point along the solution of the flow equation as one system with a different value for the leak term. In this context, a vanishing value and hence a pole in the propagator at vanishing frequency becomes meaningful again: it corresponds to a critical point where fluctuations dominate the system behavior.

The simplest measure to extract from Γ_λ is the mean value \check{x}_λ defined by the equation of state $\tilde{\Gamma}_{\check{x}, \lambda}^{(1)} [x_\lambda^*, \check{x}_\lambda^*] = 0$ [77]. Differentiating this equation with respect to λ leads to

$$\begin{aligned} 0 &= \frac{d}{d\lambda} \tilde{\Gamma}_\lambda^{(1)}(\omega) = \frac{\partial \tilde{\Gamma}_\lambda^{(1)}(\omega)}{\partial \lambda} + \int d\omega' \tilde{\Gamma}_\lambda^{(2)}(\omega, \omega') \frac{\partial}{\partial \lambda} \begin{pmatrix} \check{X}_\lambda(\omega') \\ \check{\check{X}}_\lambda(\omega') \end{pmatrix} \\ \Leftrightarrow \frac{\partial}{\partial \lambda} \begin{pmatrix} \check{X}_\lambda(\sigma) \\ \check{\check{X}}_\lambda(\sigma) \end{pmatrix} &= -\Delta_\lambda(\sigma) \left[\frac{\partial \Gamma_\lambda^{(1)}(-\sigma)}{\partial \lambda} + \frac{1}{4\pi} \frac{\partial R_\lambda}{\partial \lambda} \begin{pmatrix} \check{X}_\lambda(\sigma) \\ \check{\check{X}}_\lambda(\sigma) \end{pmatrix} \right]. \end{aligned} \quad (41)$$

To obtain (41), we have multiplied the line above by the propagator Δ_λ and used $\Delta_\lambda \tilde{\Gamma}_\lambda^{(2)} = 1$. We observe that we now need a flow equation for $\tilde{\Gamma}^{(1)}$, which we obtain by differentiating

want to renormalize all terms that also appear in the bare action. The one loop correction of $\Gamma_{\tilde{X}\tilde{X}X}^{(3)}$ ($\Gamma_{\tilde{X}\tilde{X}\tilde{X}}^{(3)}$), moreover, involves two (three) xx -propagators, so that, in systems with small fluctuations, which scale with D , this diagram is less important than the others. Compared to the one-loop correction of $\Sigma_{\tilde{X}\tilde{X}}$, $\Gamma_{\tilde{X}\tilde{X}X}^{(3)}$ bears the same number of xx -propagators, but one additional interaction, which scales with the other small factor β . Under these constraints, the non-vanishing diagrams for the self-energy are given by

$$\begin{aligned}
\frac{\partial \Gamma_{\tilde{X}X,\lambda}^{(2)}(\sigma_1, \sigma_2)}{\partial \lambda} &= \frac{1}{2} \text{diagram}_1 + \frac{1}{2} \text{diagram}_2 \\
&+ \frac{1}{2} \text{diagram}_3 \\
\frac{\partial \Gamma_{\tilde{X}\tilde{X},\lambda}^{(2)}(\sigma_1, \sigma_2)}{\partial \lambda} &= \frac{1}{2} \text{diagram}_4 + \sigma_1 \leftrightarrow \sigma_2.
\end{aligned}$$

The translation of these diagrams is shown in [Section IV K](#) where also the respective diagrams for the interaction vertex are shown. In general, the diagrams have the same form as those that appear in the fluctuation expansion, except for the presence of a single regulator in one of the propagator lines. The combination of two propagators “sandwiching” a regulator $\Delta_\lambda(q, -q) \frac{\partial R_\lambda}{\partial \lambda}(q, -q) \Delta_\lambda(q, -q)$ is called single scale propagator, because the regulator is often chosen in a way such that its derivative is peaked around frequencies with $|q| = \lambda$, thus contributing at a single scale. Due to the one-loop structure of the diagrams and the conservation of frequencies at the vertices, we have to perform one integral over an internal frequency for every possible combination of fixed external frequencies. Therefore the numerical evaluation of $\Gamma^{(n)}$ becomes increasingly computationally expensive for higher orders because at n -th order we have $n - 1$ independent external frequencies. For practical computations we thus have to truncate the hierarchy after $n = 3$ if we want to keep the full frequency dependence of $\Gamma^{(n)}$. Even at this order, the integration takes many hours on a usual desktop PC when we choose the external frequencies to range from -25 to 25 with a resolution of 0.1 . Therefore, it is legitimate to ask if one can reduce the number of required frequency-integrals by assuming a simplified frequency-dependence of higher order vertices.

1. *The BMW scheme*

A scheme that assumes a simplified momentum dependence of higher order vertices has been suggested by Blaizot, Méndez and Wschebor (BMW, [80, 81]). It has been successfully applied for example to the Kardar-Parisi-Zhang model [82]. The principal idea is to neglect the frequency-dependence of the effective action as much as possible. The most radical choice in this respect would be to assume it to be constant, which is known as the local potential approximation (LPA). BMW refined this scheme by including the exact frequency-dependence of all vertices up to a certain order s , which are functions of $s-1$ external frequencies, and to approximate vertices of the next two orders by evaluating the additional derivatives at their zero frequency-components [83]. We will pursue a different route by deriving approximate flow equations for $\Gamma^{(s+1)}$ and $\Gamma^{(s+2)}$ with the simplified frequency dependence.

More precisely, we consider a typical contribution of a vertex within the Wetterich flow equation for the vertex $\Gamma^{(s)}$ containing

$$\begin{aligned}\Gamma_\lambda^{(s+1)}(p_1, \dots, p_s + q, -q), \\ \Gamma_\lambda^{(s+2)}(p_1, \dots, p_s, q, -q),\end{aligned}\tag{45}$$

where q is the loop momentum, constrained by the regulator. For simplicity we do not specify different components of the field. The approximation assumes the vertices to depend only weakly on q and therefore sets $q = 0$ in (45), replacing the vertices by

$$\begin{aligned}\Gamma_\lambda^{(s+1)}(p_1, \dots, p_s, 0), \\ \Gamma_\lambda^{(s+2)}(p_1, \dots, p_s, 0, 0).\end{aligned}\tag{46}$$

The momentum dependence on q in the propagators and the regulator is, however, kept.

The second step of the BMW scheme allows the closure of the system: Due to the vanishing momentum on one or two legs of the vertices (46), we can express the corresponding vertex functions as the derivative of $\Gamma_\lambda^{(s)}$ with respect to a uniform (background) field $X_0^* := X^*(k=0)$:

$$\Gamma_\lambda^{(s+1)}(p_1, \dots, p_s, 0) = \frac{\delta}{\delta X_0^*} \Gamma_\lambda^{(s)}(p_1, \dots, p_s)\tag{47}$$

$$\Gamma_\lambda^{(s+2)}(p_1, \dots, p_s, 0, 0) = \frac{\delta^2}{\delta X_0^{*2}} \Gamma_\lambda^{(s)}(p_1, \dots, p_s).\tag{48}$$

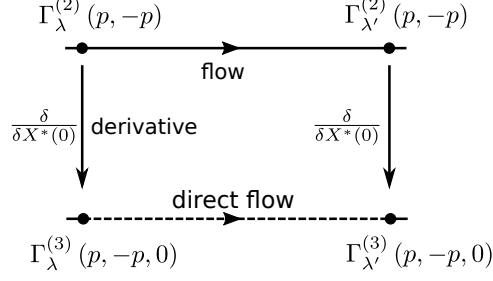


Figure 4. Implementation of the BMW scheme within the vertex expansion. In the original formulation (top) we have to evaluate the derivatives $\delta/\delta X^*(0)$ numerically at each λ . In our interpretation (bottom) we derive an additional flow equation for $\Gamma^{(3)}(p, -p, 0)$ (dashed line).

If we now use (47) and (48) to replace $\Gamma_\lambda^{(s+1)}$ and $\Gamma_\lambda^{(s+2)}$ by the ordinary derivatives of $\Gamma_\lambda^{(s)}$ with respect to the zero-modes of X, \tilde{X} , we close the set of flow equations and additionally we take into account the flow of order $s+1$ and $s+2$, at least approximately. Since we reduced the number of independent momenta by one (or two, respectively), the computation time decreases significantly.

But the resulting equation is a partial differential equation in λ and X_0^* [83, eq. (19)]; we hence have to evaluate the derivatives with respect to X_0^* for every step at which we compute $\partial_\lambda \Gamma^{(s)}$. Below we describe an alternative scheme that circumvents this complication and entirely stays within the realm of a vertex expansion.

2. Removing the PDE

We aim to apply the BMW approximation at order $s = 2$, thus keeping the full momentum dependence of the self-energy. However, within the vertex expansion scheme it remains unclear how to compute the derivatives of $\Gamma^{(2)}$ numerically. This is because at each given λ we know the value of $\Gamma^{(2)}$ only for the true mean value $\phi = \tilde{X}_\lambda(0)$, but not in a vicinity around it; we therefore cannot approximate the derivative by a quotient built from finite differences.

We can circumvent this problem by deriving an additional flow equation for $\Gamma_\lambda^{(3)}(p_1, p_2, 0)$ (illustrated in Figure 4; the more complex situation with x and \tilde{x} fields will be addressed below) and in principle also for $\Gamma_\lambda^{(4)}(p_1, p_2, 0, 0)$, which we neglect in our model. We obtain this flow equation by differentiating the flow equation for $\Gamma_\lambda^{(2)}$ with respect to $X^*(0)$, i.e.

$\frac{\delta}{\delta X^*(0)} \partial_\lambda \Gamma_\lambda^{(2)} = \partial_\lambda \Gamma_\lambda^{(3)}$ and then setting those momenta of the original three-point vertices to zero that are connected to the single scale propagator, in line with the BMW scheme. But we need to keep the dependence on q of the vertices that emerge when we differentiate a propagator by the background field. Otherwise we would make an additional approximation on top of BMW. Thus, drawing only the first argument of the propagators, in diagrammatic language we obtain

$$\frac{\delta}{\delta X(0)} \frac{\partial \Gamma_\lambda^{(2)}(p_1, p_2)}{\partial \lambda} = \frac{\delta}{\delta X(0)} \frac{1}{2} \text{Diagram (1)(2)}$$

$$\stackrel{\text{BMW}}{=} -\frac{1}{2} \text{Diagram (3)(4)(5)} - \frac{1}{4} \text{Diagram (6)(7)(8)} - \frac{1}{2} \text{Diagram (9)(10)}$$

$+ p_1 \leftrightarrow p_2$

where the vertex functions are given by

$$\begin{aligned} (1) : \Gamma_\lambda^{(3)}(p_1, q, -p_1 - q) & \quad (2) : \Gamma_\lambda^{(3)}(p_2, -q, p_1 + q) \\ (3) : \Gamma_\lambda^{(3)}(p_1, 0, -p_1) & \quad (4) : \Gamma_\lambda^{(3)}(p_2, 0, -p_2) & \quad (5) : \Gamma_\lambda^{(3)}(q, -q, 0) \\ (6) : \Gamma_\lambda^{(3)}(p_1, 0, -p_1) & \quad (7) : \Gamma_\lambda^{(3)}(p_2, 0, -p_2) & \quad (8) : \Gamma_\lambda^{(3)}(p_1 + q, -p_1 - q, 0). \\ (9) : \Gamma_\lambda^{(4)}(p_1, 0, -p_1, 0) & \quad (10) : \Gamma_\lambda^{(3)}(p_2, 0, -p_2) \end{aligned}$$

The crucial point to notice is that all vertices that appear in the diagrams have only two nonzero momenta. The set of differential equations is therefore closed, if we neglect the last diagram that contains a four point vertex. So we have found an explicit flow equation for $\Gamma_\lambda^{(3)}(p_1, p_2 = -p_1, 0)$, indicated by the dashed line in [Figure 4](#). As a consequence we have to solve a coupled set of ODEs instead of a PDE.

If we do not want to neglect the flow of the four point vertex completely, we can differentiate the diagrams once again, which leads to a flow equation of $\Gamma_\lambda^{(4)}(p_1, p_2, 0, 0)$. This flow equation then depends on $\Gamma_\lambda^{(3)}(p_1, p_2, 0)$, $\Gamma_\lambda^{(4)}(p_1, p_2, 0, 0)$ and $\Gamma_\lambda^{(5)}(p_1, p_2, 0, 0, 0)$. Due

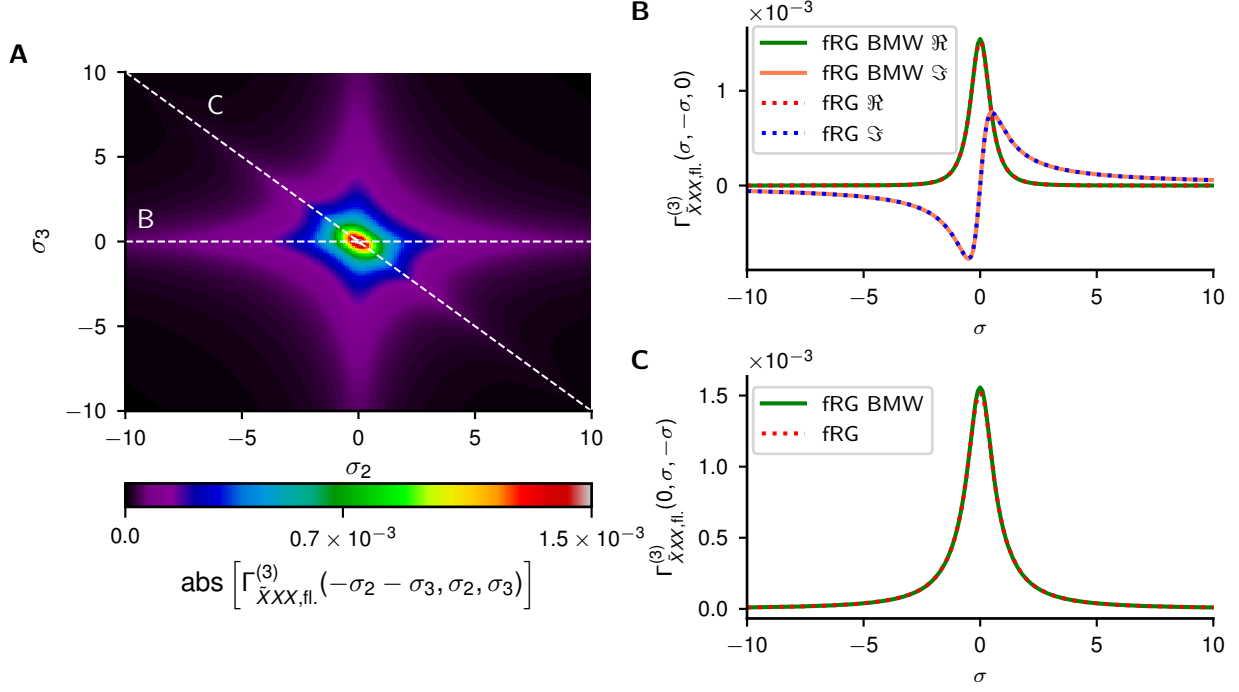


Figure 5. $\Gamma_{\tilde{xxx},\text{fl.}}^{(3)}$ computed by fRG schemes. (A) shows the full frequency dependence as a result of the calculation where we take into account the flow of the mean value, $\Gamma_{\text{fl.}}^{(2)}$, and $\Gamma_{\tilde{xxx},\text{fl.}}^{(3)}$. Panels (B) and (C) show $\Gamma_{\tilde{X}XX,\lambda,\text{fl.}}^{(3)}(-\sigma_2 - \sigma_3, \sigma_2, \sigma_3)$ along the sections $\sigma_3 = 0$ (B) and $\sigma_2 = -\sigma_3$ (C) which are indicated by the white dashed lines in (A) and compare it to the respective types of vertices that appear in the BMW approximation. Note that $\Gamma_{\tilde{X}XX,\lambda,\text{fl.}}^{(3)}(0, \sigma_2, -\sigma_2) \in \mathbb{R}$ because its Fourier transform $\Gamma_{\tilde{xxx},\lambda,\text{fl.}}^{(3)}(0, t_2, -t_2)$ is real by definition and symmetric because the last two arguments are those of two x 's at different time points, which are interchangeable.

to the emergence of the latter, the set of equations can be closed only if we truncate the series at some order (unlike the original BMW scheme).

Figure 5 compares the three point vertices obtained from the truncated flow equation to the result from the BMW approximation. The latter of course only yields the three-point vertex $\Gamma_{\tilde{X}XX}^{(3)}(\sigma_1, \sigma_2, \sigma_3)$ along the one-dimensional sections $-\sigma_1 = \sigma_2 + \sigma_3 = 0$ and $\sigma_3 = 0$. The agreement between the two approximations is high. This result is to be expected, since the fluctuation corrections per se are small in the regime considered, so that the bare vertices still constitute the largest contributions to any fluctuation correction.

III. DISCUSSION

This article surveys methods to obtain self-consistent approximations by means of functional and diagrammatic techniques for stochastic differential equations as they appear in models of neuronal networks. Besides a systematic introduction, going from simple to more complex methods, we present three main new findings.

First, we expose the fundamental relation between the Onsager-Machlup (OM) effective action, which has a direct physical interpretation, and the Martin - Siggia - Rose - De Dominicis - Janssen (MSRDJ) effective action, which is computationally favorable. The general exposition of this fundamental link, to our knowledge, has been missing in the literature; it has earlier surfaced in specific problems in certain approximations [63]. In particular, the derivation of the OM effective action from the corresponding MSRDJ effective action naturally extends the definition of the former beyond Gaussian noise.

Second we consider two effective equations that are equivalent to the stochastic nonlinear system. The first is a deterministic integro-differential equation that captures the time evolution of the mean of the process. A similar equation has previously been derived within the Doi-Peliti formalism of Markovian dynamics [64]. The second is a stochastic, but linear integro-differential equation that has identical second order statistics as the full system. These effective equations serve us here to provide an intuitive interpretation of the meaning of various vertex functions and to show how to relate stochastic nonlinear models to effective deterministic or stochastic linear systems.

Third, we develop a truncation scheme for the hierarchy of flow equations that arises in the functional renormalization group, which is based on the BMW scheme [80]. We here transfer this method from the derivative expansion to the vertex expansion, and demonstrate that this scheme yields a closed set of flow equations for the vertex functions which accurately captures the statistics of the system. The presented scheme is generic and may therefore be employed beyond the application to neuronal dynamics.

The model system studied in the current manuscript is admittedly simple and is mostly meant to illustrate the techniques in a minimal setting. In the following we would therefore like to provide a slightly wider outlook for potential applications that are of relevance to the study of neuronal networks.

The initial part of this manuscript reformulates the problem of finding self-consistency

equations by help of the effective action. We here apply the standard approach known from quantum field theory and statistical physics [59]. This technique yields self-consistent equations for the mean of the process that incorporate fluctuation corrections. Potential applications to neuronal networks include the study of bifurcations in the network dynamics. Pitchfork bifurcations, for example, are responsible for the occurrence of multi-stability, the basis of classical attractor networks [12]. The effective action allows us to transfer the concept of a bifurcation in a deterministic differential equation [84] to a stochastic system: We need to investigate the bifurcations of the stationary points of the effective action, instead of studying the differential equation itself. A pitchfork bifurcation, the transition from a regime with a unique solution to a one with multiple fixed points, corresponds in the stochastic system to a critical point; the effective action changes from having a single minimum to exhibiting a flat segment that, beyond the bifurcation point, admits a continuum of stationary states. Traversing the bifurcation point, the curvature vanishes and hence fluctuations diverge. We here showed that the Onsager-Machlup effective action clearly exposes this fundamental property. Beyond the transition point, the system may be brought to jump from one end of the plateau to the other - showing a first order phase transition as an external parameter is varied.

The study of transitions to oscillatory states, as they are ubiquitously observed in neuronal systems [85], would require the computation of the effective action as a functional of a field with Fourier components at non-zero frequencies. If the stationary point of the functional is assumed at a constant field configuration at one side of the bifurcation and by an oscillatory state on the other side, we have the stochastic analogue of a Hopf bifurcation. These bifurcations play a central role for the generation of oscillations [86] and for the appearance of spatio-temporal waves which are observed in cortical networks [87, 88]. The formalism exposed here makes the influence of noise on such bifurcations accessible. For example, the recently found second order phase transition at the onset of an oscillatory state [89] could be analyzed within this framework. Studying bifurcations in neuronal networks in the presence of symmetries, techniques based on the equivariant branching lemma have recently been applied to neuronal networks [90]. So far these techniques neglect the influence of the noise altogether (i.e. employ the tree-level approximation) and therefore their applicability, at best, is limited to network states with weak noise. The formulation of bifurcations in terms of the effective action would allow an extension of this method to

study how symmetries constrain bifurcations between fluctuation-dominated states.

A closely related point is the transition between multiple stable states, such as up- and down states [91, 92] or the different states of an attractor network [12]. The average noise-driven paths of transitions between such meta-stable states allows the assessment of the statistics of transitions between multiple states, for example to quantify the vulnerability to noise of information encoded in the activation of an attractor. Technically, one here seeks escape solutions to the equation of state which have non-vanishing values for the response field \tilde{x} [93, 94][see 95, i.p. Chapter 10 for a review]. The loop expansion and the functional renormalization group can be used to compute such average escape paths. What is required, though, is the computation of the effective action $\Gamma[x, \tilde{x}]$ also for non-vanishing values of the response field \tilde{x} . Alternatively one may compute its derivatives, the vertex functions $\Gamma^{(n)}$, including derivatives by \tilde{x} at vanishing background field $\tilde{x} \equiv 0$. The functional Taylor representation of Γ then serves as an approximation around the classical non-escape path that can be evaluated for small deviations $\delta\tilde{x} \neq 0$. We demonstrated the utility of this latter approach in the computation of the effective equation of motion for the mean value in the setting of given initial value and free endpoint (relaxation). The theoretical prediction agrees with the simulation reasonably well. A related approach was here used to provide an approximation for the effective potential: If the approximation of the MSRDJ effective action is quadratic in the response field, taking the supremum over \tilde{x} is equivalent to integrating out the response field to obtain the OM effective action. This technique has an advantage over the computation of $\Gamma[x, \tilde{x}]$ for arbitrary values of $\tilde{x} \neq 0$, because in the latter case closed response loops do not vanish, neither do the propagators $\Delta_{\tilde{x}\tilde{x}}$, thus proliferating the number of diagrams to compute.

The loop expansion is shortly reviewed here, because it provides qualitative insights into the leading order of the fluctuation corrections. In the context of neuronal networks, the seminal work by Buice and Cowan [69] has introduced this technique to the study of neuronal networks. Since the structure of the one-loop diagrams is identical to those that appear in the functional renormalization group, one may use this method to check which additional vertices are produced along the RG flow, thus providing information for a good ansatz for the effective action. We here show that the loop expansion for the considered example is an expansion $\propto \beta^2 D$, where D is the amplitude of the noise and β the prefactor of the nonlinearity. In our example, fluctuations are small so that the one-loop result is

already quite accurate. The sign of the fluctuation corrections together with the form of the effective equations for the mean and for the second order fluctuations, moreover expose qualitative mechanisms that arise from the fluctuation corrections: We show that a convex non-linearity always causes a positive shift of the mean of the process and that the additional linear memory kernel that arises from the self-energy has a sign that diminishes the leak term, thus causing a slower relaxation of the system - the interplay of noise and non-linearity thus prolongs the memory of a stimulus within the system. For small deflections from the steady state, this indirect contribution, moreover, typically dominates over the effect of the nonlinearity per se. Correspondingly we show that the power spectrum at low frequencies is enhanced. Convex non-linearities of the gain functions of neurons are typical in regimes in which neurons are driven by fluctuations [10].

The functional renormalization group (fRG) approach is presented here in the context of neuronal dynamics as a method that overcomes the limitations of the loop expansion with regard to self-consistency that is restricted to the mean. Instead, all vertex functions are potentially renormalized by fluctuation corrections, thus in principle allowing a full self-consistent treatment also including corrections to the propagators and the interaction vertices. In the regime of weak fluctuations, we show that the results are slightly superior to the one-loop approximation, but here do not yield qualitatively new results. Computing higher order loop approximations is, moreover, inherently difficult, whereas all integrals in the fRG approach always have one-loop structure. The fRG-approach, however, leads to improved results over the one-loop-approximation even though the frequency-resolution of higher order vertices is limited by the adapted BMW-approximation introduced here. Given in addition that similar ansätze have been successfully applied to spatially extended systems like the KPZ-model [82], we believe that the insights gained by this work will prove useful in studying neuronal networks embedded in space. Here, also more sophisticated approaches might become useful, for example the decomposition of vertices in so-called channels, characterized by the way they can be separated into two pieces by cutting two lines (particle-particle, particle-hole and crossed particle-hole in solid state physics terms). For a momentum-independent bare interaction, the contribution of each channel has a characteristic momentum structure, which can be used to drastically reduce the numerical effort both in fRG [96, 97] and parquet calculations [98].

While in the fRG, the effect of higher order statistics on lower orders can be accounted

for systematically, many studies of neuronal networks neglect this feedback, and keep the nonlinear terms at their mean field level. This approach has been shown to yield good results [99, eq. (6)], [100, eq. (3.8)] if fluctuations are not too strong. This is in line with our results provided that the noise level is low, because the linear memory kernel scales with $D\beta^2$, as can be seen in (34). Therefore for $D\beta^2 \ll 1$, while $\beta = \mathcal{O}(1)$, it might indeed be sufficient to consider the deterministic effect of the nonlinearity, but not the interaction with the noise. However, for $D\beta^2 = \mathcal{O}(1)$ while $\beta \ll 1$, the nonlinear effects by themselves are negligible, but their interaction with the noise induces a significant memory term. Setting β exactly to zero obviously makes both effects vanish, which might lead to the erroneous conclusion that the nonlinearity without the noise is the reason for the deviation from the linear case.

From a conceptual point of view, the functional renormalization group is interesting, because the flow generates new interaction vertices that are not contained in the original model. Thus, this method shows how the description of a neuronal network changes from one scale to another: It exposes which effective interactions are generated by the interplay of nonlinearities and fluctuations. A specific feature of a flat regulator in frequency domain is its direct physical interpretation as a leak term of the neuronal dynamics. Thus it controls the bare relaxation rate towards equilibrium. Each point along the renormalization group flow therefore corresponds to one physical system with a different value of the relaxation term. This insight may be used to study the approach towards a critical point at which the leak term vanishes and the time scale of fluctuations diverges. Despite its simplicity, the here-considered model exposes two fundamental properties: First, the fluctuation corrections to the self-energy $\Sigma_{\bar{x}x}$ shift the point of transition with regard to mean-field theory. The latter predicts criticality at the point of vanishing leak term $m = 0$. The self-energy corrections reduce the leak term, thus promoting critical fluctuations. The critical point is therefore reached already at a non-zero negative value $m_c < 0$ of the leak term. Qualitatively, the behavior of the self-energy corrections is therefore opposite to the best known text book model of criticality, the φ^4 theory, where the transition is delayed to a negative mass term [e.g. 61, eq. 6.26]. In addition, a second mechanism causes a shift of the transition point, which is absent in an even theory as the φ^4 model: Fluctuation corrections to the mean value increase the mean value \bar{x} . Thus, the effective leak term $m(\bar{x})$ is weakened, further promoting the approach to the critical point.

These generic observations only depend on the assumption of an expansive non-linear

neuronal gain function. Even though the model system studied here is admittedly simple, it yet illustrates these features that we also expect for example in a (fully or densely connected) network. The shift of the transition point obviously depends on the amplitude of the noise. It is known that fluctuations vary in neuronal networks in response to stimuli [101, 102]. Thus, neuronal systems may dynamically change their distance to the critical point within short periods of time.

A particularly interesting feature of the approach to the critical point are trajectories that depart from the stationary mean towards the location of the second, unstable, fixed point. Their dynamics slows down not only due to the reduced leak term by the two mechanisms described above, but also due to passing the vicinity of the second, unstable fixed point. In neuronal systems this mechanism may be useful to generate transient behavior on slow time scales, beyond the slow down of fluctuations close to the stable fixed point. One may speculate if such mechanisms play a role in long transient behavior observed in delayed response tasks [103].

Recently a Ginzburg-Landau type theory of neuronal activity has been formulated by DiSanto et al. [89]. A bit earlier, Henningson and Illes [104] succeeded in fitting a simpler, linear model - a leaky heat equation with additional Gaussian noise - to the recordings of subthreshold fluctuations in acute hippocampal brain slices from a rat. Such models, expressed as partial stochastic differential equations, naturally fall into the realm of the statistical field theoretical methods discussed here. In particular the study of second order phase transitions has come into reach now. Either by employing the established formalism of statistical field theory based on Wilson's renormalization group for non-equilibrium stochastic dynamics [see 5, for an authoritative review] or by the functional renormalization group methods presented here. Whether or not non-trivial fixed points in neuronal networks are accessible by former methods that rely on the closeness of the fixed point to a Gaussian one is so far unclear. The closely related Kardar-Parisi-Zhang model [105], for example, exhibits fixed points in the strong coupling regime, which is therefore only accessible by non-perturbative methods, for example the fRG approach presented here [106].

The currently employed theory of second order phase transitions in neuronal networks follows two main themes. First, the idea of a branching parameter, the average number of downstream descendants produced by the current activity [107, 108]. It relates second order phase transitions to the transition originally studied in the sandpile model [109]. Second, the

comparison of experimentally measured activity to equilibrium ensembles, such as pairwise maximum entropy models [110, 111]; the discrepancy between the non-equilibrium dynamics of neuronal networks and this latter approach based on equilibrium thermodynamics has been identified as a pressing problem [112]. Following a field theoretical approach would in particular allow the study of critical exponents in models where neuronal activity unfolds in a spatially extended field, representing a coarse-grained view on the activity of mesoscopic numbers of neurons at each space point. Thus it would enable experimental predictions, for example with regard to the spatial structure of correlated activity. For the Manna sandpile model [113] such a continuous theory has been formulated and it has been found to belong to the universality class of directed percolation with a conserved quantity (C-DP) [114–116]; the conservation of the number of sand grains here gives rise to the conserved quantity. Belonging to the C-DP universality class, the Manna sandpile model in particular features an absorbing state. In neuronal networks, though, we typically see ongoing activity; the absence of an absorbing state would therefore give rise to a different structure of the effective field theory, possibly also affecting the universality class. An alternative approach is therefore to start at the biophysics of neuronal networks on the microscopic level and to derive the structure of an effective long-range field theory. Investigating such models, the functional renormalization group has proven one of the few tools that make non-perturbative RG fixed points accessible [117].

So far field theoretical methods have been applied to neuronal networks with Markovian dynamics on discrete state spaces [69, 118], employing the Doi-Peliti [70] formalism or the alternative approach by Lefèvre and Biroli [119, 120], which is closer to the MSRDJ formulation used here. Also neuronal dynamics described by stochastic differential equations [7, 8, 45, 121–123] and stochastically spiking models (non-linear Hawkes processes [124, 125]) have recently been formulated by field theoretical methods [126]. For leaky integrate-and-fire models in the mean driven regime, a mapping to a coupled set of phase oscillators, moreover, allows the application of the MSRDJ formalism [127, 128]. The renormalization group methods that we presented here can directly be applied to these systems.

Networks of leaky integrate-and-fire models [129] in the fluctuation driven, asynchronous irregular state [10, 11] are, however, inherently complicated to treat by field theoretical methods; the reason is that an action for such models is cumbersome to define due to the hard threshold and reset of the membrane potential. This model and its biophysically more

realistic extensions [130], however, form a kind of gold standard. It would therefore be a major step to treat networks of such models by systematic approaches as they are offered by field theory. So far methods for this central model are constrained to ad-hoc mean-field approximations, typically resting on the annealed approximation of the connectivity [11, 131]; in particular this mean-field based approach prohibits a systematic study of critical phenomena.

In summary, the current work imports methods from established fields of physics into the field of theoretical neuroscience that we think have a high potential to solve some of the technical difficulties that arise in the study of neuronal networks in the presence of fluctuations, non-linearities, phase transitions, and critical phenomena.

ACKNOWLEDGMENTS

We thank PierGianLuca Porta Mana for fruitful discussions.

This work was partly supported by the Exploratory Research Space seed funds MSCALE and CLS002 (partly financed by Hans Herrmann Voss Stiftung) of the RWTH university; the JARA Center for Doctoral studies within the graduate School for Simulation and Data Science (SSD); the Helmholtz association: Young investigator’s grant VH-NG-1028; European Union’s Horizon 2020 Framework Programme for Research and Innovation under the Specific Grant Agreement No. 785907 (Human Brain Project SGA2); Juelich Aachen Research Alliance (JARA).

IV. APPENDIX

A. Euler Lagrange equation for the most likely path

We want to find the most likely path between an initial point $x(0) = x_0$ and a final point $x(T) = x_T$. This leads to the Euler Lagrange equation by a straight forward calculation: We consider the variation of the action (5) with regard to all variations of the path $x(t) + \delta x(t)$, where the variation vanishes on the end-points, which is $\delta x(0) = \delta x(T) = 0$. By Taylor

expansion we get

$$\begin{aligned} & \int L(x(t) + \delta x(t), \dot{x}(t) + \delta \dot{x}(t)) dt \\ &= \int L(x(t), \dot{x}(t)) + \partial_x L(x(t), \dot{x}(t)) \delta x(t) + \partial_{\dot{x}} L(x(t), \dot{x}(t)) \delta \dot{x}(t) dt + O(\delta^2) \end{aligned}$$

Applying integration by parts to the latter term we get

$$\int \partial_{\dot{x}} L(x(t), \dot{x}(t)) \delta \dot{x}(t) dt = - \int \frac{d}{dt} \{ \partial_x L(x(t), \dot{x}(t)) \} \delta x(t) dt,$$

where the boundary term vanishes due to the fixed end points of $\delta x(0) = \delta x(T) \equiv 0$.

So requesting stationarity for all possible variations δx we need to have that

$$0 = \frac{d}{dt} \{ \partial_x L(x, \dot{x}) \} - \partial_x L(x, \dot{x}), \quad (49)$$

which is just the Euler-Lagrange equation known from classical mechanics.

B. Normalization and escape

It is often stated that in stationary settings all moments of the response field vanish [55, p. 38][56]. This statement follows from the normalization of the probability functional $p[x|\tilde{j}]$ for all paths, $\int \mathcal{D}x p[x|\tilde{j}] = 1$. The latter is given by

$$p[x|\tilde{j}] = \int \mathcal{D}\tilde{x} \exp(S[x, \tilde{x}] + \tilde{j}^T \tilde{x}). \quad (50)$$

The normalization can therefore also be written as $Z[0, \tilde{j}] \equiv 1$, which, upon n -fold differentiation by \tilde{j} , yields

$$\langle \tilde{x}(t_1) \cdots \tilde{x}(t_n) \rangle \equiv 0 \quad \forall t_1, \dots, t_n, n. \quad (51)$$

However, we found above for escape solutions in (13) that $\tilde{x} \neq 0$, which implies that at least one moment of \tilde{x} is unequal to zero. How is this possible?

The problem of fluctuation-driven paths can be quite generally rephrased like this: The coupled set of differential equations (11) and (12) has a unique solution if one fixes the initial condition $(x(0), \tilde{x}(0))$; in particular, the end point $x(T)$ at time T is fixed. Alternatively, we may specify the initial point $x(0)$ and the final point $x(T)$. The form of (12)

$$\partial_t x = f(x) - D\tilde{x}$$

is identical to the deterministic part with an additional inhomogeneity due to the term $D\tilde{x}$. If we fix an initial and a final point so that these two points are not connected by the solution of the deterministic part alone, $\tilde{x}(t') \neq 0$ must be non-zero for at least one point $t' \in [0, T]$. Since the equation (11) for \tilde{x} is linear and we assume f to be smooth, this implies that $\tilde{x}(t) \neq 0 \quad \forall t \in [0, T]$. In summary we see that departures of the evolution of x from its deterministic behavior necessarily imply $\tilde{x} \neq 0$.

The apparent contradiction between (51) and the solution of (13) with nonzero $\tilde{x}^*(t)$ is resolved as follows. The normalization condition of (50) results from the integration over the entire space of trajectories. The argumentation implicitly assumes that we specify the initial point of the process $x(0)$; integrating over all following time points in the normalization condition then naturally yields unity; it is just a consequence of conservation of probability.

If, on the other hand, we specify the end point of the path, we implicitly restrict the ensemble of paths in the integral appearing in Z . In the path integral formulation, we include the initial point x_0 and the final point x_T as

$$\mathcal{Z}[j, \tilde{j}] = \int \mathcal{D}x \int \mathcal{D}\tilde{x} \exp(S[x, \tilde{x}] - \tilde{x}^T \delta(\circ) x_0 + j^T x + \tilde{j}^T \tilde{x}) \delta(x(T) - x_T).$$

The presence of the initial condition x_0 obviously does not affect the normalization - it can as well be absorbed into a shift of $\tilde{j} \rightarrow \tilde{j} - \delta(\circ)x_0$. Fixing the final condition x_T , however, leads to the relation

$$\mathcal{Z}[0, \tilde{j}] = p(x(T) = x_T | x_0, \tilde{j}),$$

which is the conditional probability to reach the final point x_T from the initial point x_0 given the inhomogeneity \tilde{j} . This probability is not necessarily independent of \tilde{j} - for example a negative inhomogeneity \tilde{j} in the stochastic differential equation may elevate the probability to ultimately reach a larger x_T . A properly normalized moment-generating functional $Z[j, \tilde{j}] = \mathcal{Z}[j, \tilde{j}] / \mathcal{Z}[0, 0]$ yields moments of the ensemble, but does not affect the latter conclusion - we will have $\langle \tilde{x}^n \rangle = \delta^n Z / \delta \tilde{j}^n \neq 0$ in general. Thus, there is no contradiction to the theorem that all moments of \tilde{x} be zero due to normalization; in particular we may have a non-zero first moment of the response field $\tilde{x}^*(t) \equiv \langle \tilde{x}(t) \rangle$.

The form of the equations of state (11) and (12) are, however, the same for both ensembles, because they arise by varying the trajectory only in the open interval $(0, T)$; they are not affected by fixing the starting or end point. The latter only provide the boundary conditions for the solutions to these equations.

To conclude let us explain why solutions of the tree-level equations of state with $\tilde{x} = 0$ are distinguished and we therefore consider them separately in [Section II C](#). Explicitly performing the supremum in (14), we obtain

$$\tilde{x} = \frac{f(x) - \dot{x}}{D},$$

so that we can rewrite the Onsager-Machlup action as

$$- \int_{t_i}^{t_f} \frac{(f(x(t)) - \dot{x}(t))^2}{2D} dt = - \int_{t_i}^{t_f} \frac{D}{2} \tilde{x}(t)^2 dt.$$

Because the left hand side is the exponent of the probability of the path $x(t)$, we see that $\tilde{x}(t) = 0 \forall t$ is the solution with the highest probability. By setting \tilde{x} identically to zero, we limit ourselves to a lower-dimensional subspace of the entire phase space so that we are just allowed to chose either the initial or the final point and the respective other one is determined by this choice. This is also intuitively expected from the average of a relaxation process as described in [Section II C](#).

C. General properties of the effective action in the MSRDJ-formalism

Multiple derivatives of Γ with respect to x are always zero, as we will demonstrate in this section. We have seen in [Section IV B](#) that if we do not specify an endpoint for x , the expectation value of all powers of \tilde{x} vanish. As a consequence, we see from (24) that $\Gamma_{xx}^{(2)}[x^*, 0] = 0$. Extending our analysis to higher order derivatives of Γ not involving \tilde{x} , we observe that

$$\begin{aligned} \Gamma_{xxx}^{(3)} &= \sum_{y \in \{x, \tilde{x}\}} \sum_{y_1, y_2, y_3} \Gamma_{x_1 y_1}^{(2)} \Gamma_{x_2 y_2}^{(2)} \Gamma_{x_3 y_3}^{(2)} W_{y_1, y_2, y_3} \\ &\stackrel{\Gamma_{x\tilde{x}}^{(2)}=0}{=} \sum_{\tilde{x}_1, \tilde{x}_2, \tilde{x}_3} \Gamma_{x_1 \tilde{x}_1}^{(2)} \Gamma_{x_2 \tilde{x}_2}^{(2)} \Gamma_{x_3 \tilde{x}_3}^{(2)} \underbrace{W_{\tilde{x}_1, \tilde{x}_2, \tilde{x}_3}}_{=0} = 0. \end{aligned} \quad (52)$$

Similarly, we can argue for all higher order vertices: They can be decomposed into “tree diagrams” with derivatives of W as nodes and $\Gamma^{(2)}$ as connecting elements. A tree diagram is defined by having the property that it does not include loops and especially, two nodes are connected by exactly one element $\Gamma^{(2)}$. Because we have only x ’s at the external legs and $\Gamma_{xx}^{(2)} = 0$, we have all but one of the derivatives of a $W^{(n)}$ connected to external legs to be with respect to \tilde{j} . Because the external legs by construction are therefore attached

to \tilde{j} -derivatives, the only possibility to “justify” j -derivatives are $\Gamma_{x\tilde{x}}^{(2)}$ -components acting as internal connecting elements providing one j -derivative each. Since the graphs are tree-like, we have exactly one $W^{(n)}$ -node more than connecting elements. However, we need at least one j -derivative at every node to prevent that it vanishes. We deduce that the contribution of at least one of the nodes vanishes. This demonstrates that

$$\Gamma_{\underbrace{x, \dots, x}_{n \text{ times}}}^{(n)} = 0 \quad \forall n.$$

D. The effective action in the MSRDJ and the Onsager-Machlup-formalism

Considering Γ as a potential whose extremal points are the solutions of a differential equation and that $\tilde{x} = 0$ is the extremizing solution, we might conclude from $\Gamma_{x\dots x}^{(n)} = 0$ (shown in (52)) that Γ is constant (or at least nonanalytic in $(\tilde{x}, 0)$). However, Γ is clearly non-constant. It turns out that setting $\tilde{x} = 0$ is correct for the stationary point \tilde{x} , but does not give us the true shape of the “energy landscape” for a different x in a neighborhood of \tilde{x} . The reason for this is that it is forbidden to set \tilde{x} to a constant value prior to the calculation of the statistics of x ; instead we must integrate it out, since it is just a Hubbard-Stratonovich auxiliary field used to formulate a constraint. Only for Gaussian noise, this leads to the Onsager-Machlup-action (5). For arbitrary noise distributions, we can define the cumulant-generating function without the need to first define the OM-action by writing

$$W_{\text{OM}}[j] = \ln \int \mathcal{D}x \int \mathcal{D}\tilde{x} \exp(S[x, \tilde{x}] + j^T x) \quad (53)$$

This makes sense because we introduced \tilde{x} as an auxiliary variable to represent the delta-distribution and \tilde{j} to measure the response function. If we are not interested in the latter, but just in the statistics of x , we can drop \tilde{j} in (20) to obtain (53). The Onsager-Machlup-type effective action then takes the form

$$\begin{aligned} \Gamma_{\text{OM}}[x^*] &= \sup_j j^T x^* - W_{\text{OM}}[j] \\ &= [j^T x^* - W_{\text{OM}}[j]]_j \text{ such that } x^* = \frac{\partial}{\partial j} W_{\text{OM}}[j]. \end{aligned}$$

Let us expose the connection to the MSRDJ-formalism more clearly by performing the Legendre transform with respect to j and \tilde{j} gradually instead of simultaneously:

$$\begin{aligned}\Gamma_1[x^*, \tilde{j}] &:= \sup_j j^T x^* - W[j, \tilde{j}] \\ \Gamma_2[x^*, \tilde{x}^*] &:= \sup_{\tilde{j}} \tilde{j}^T \tilde{x}^* + \Gamma_1[x^*, \tilde{j}].\end{aligned}$$

We easily see that $\Gamma_{\text{OM}}[x] = \Gamma_1[x, 0]$. For the identification of Γ_2 , observe that for the elimination of j obtaining Γ_1 , we choose $j[x, \tilde{j}]$ such that

$$x = \frac{\partial}{\partial j} W[j[x, \tilde{j}], \tilde{j}]$$

and in the second step, yielding Γ_2 , we determine \tilde{j} in the following way:

$$\begin{aligned}\tilde{x} &= -\frac{d}{d\tilde{j}} \Gamma_1[x, \tilde{j}] = -\frac{d}{d\tilde{j}} \{j[x, \tilde{j}]x - W[j[x, \tilde{j}], \tilde{j}]\} \\ &= -\frac{\partial j}{\partial \tilde{j}} x + \underbrace{\frac{\partial W}{\partial j}[j[x, \tilde{j}], \tilde{j}]}_{=x} \frac{\partial j}{\partial \tilde{j}} + \frac{\partial W}{\partial \tilde{j}}[j[x, \tilde{j}], \tilde{j}] = \frac{\partial W}{\partial \tilde{j}}[j[x, \tilde{j}], \tilde{j}],\end{aligned}$$

which leads to the identification $\Gamma_{\text{MSRDJ}}[x, \tilde{x}] = \Gamma_2[x, \tilde{x}]$. Therefore, we obtain Γ_{OM} by performing the Legendre transform of Γ_{MSRDJ} with respect to \tilde{x} and setting $\tilde{j} = 0$ afterwards, which is equivalent to finding the \tilde{x} extremizing $\Gamma_{\text{MSRDJ}}[x, \tilde{x}]$ for given x , or, in other words,

$$\Gamma_{\text{OM}}[x^*] = \sup_{\tilde{x}} \Gamma_{\text{MSRDJ}}[x^*, \tilde{x}] =: \sup_{\tilde{x}} \Gamma[x^*, \tilde{x}].$$

1. Second derivative of the effective potential

Using the definition of the effective potential

$$\begin{aligned}\Gamma_{\text{OM}}[x] &:= \Gamma_{\text{MSRDJ}}[x, \tilde{x}[x]], \text{ where } \tilde{x}[x] \text{ is defined by} \\ \frac{\delta}{\delta \tilde{x}(t)} \Gamma_{\text{MSRDJ}}[x, \tilde{x}[x]] &= 0\end{aligned}$$

we obtain an explicit expression for $\frac{\delta x}{\delta \tilde{x}}$ by evaluating the derivative

$$\begin{aligned}
0 &= \frac{\delta}{\delta x(t)} \frac{\delta}{\delta \tilde{x}(s)} \Gamma_{\text{MSRDJ}} [x, \tilde{x} [x]] \\
&= \frac{\delta^2}{\delta x(t) \delta \tilde{x}(s)} \Gamma_{\text{MSRDJ}} [x, \tilde{x}] \Big|_{\tilde{x}=\tilde{x}[x]} + \int ds' \frac{\delta^2}{\delta \tilde{x}(s') \delta \tilde{x}(s)} \Gamma_{\text{MSRDJ}} [x, \tilde{x}] \Big|_{\tilde{x}=\tilde{x}[x]} \frac{\delta \tilde{x}(s')}{\delta x(t)} [x]
\end{aligned} \tag{54}$$

$$\Leftrightarrow \frac{\delta \tilde{x}(s')}{\delta x(t)} [x] = - \int ds'' \left[\frac{\delta^2}{\delta \tilde{x} \delta \tilde{x}} \Gamma_{\text{MSRDJ}} [x, \tilde{x}] \Big|_{\tilde{x}=\tilde{x}[x]} \right]_{s's''}^{-1} \frac{\delta^2}{\delta \tilde{x}(s'') \delta x(t)} \Gamma_{\text{MSRDJ}} [x, \tilde{x}] \Big|_{\tilde{x}=\tilde{x}[x]} . \tag{55}$$

Note for the first step that the derivatives in the first line are total ones, but the one with respect to \tilde{x} only affects the second argument of Γ_{MSRDJ} , whereas the one with respect to x affects both arguments. In the second line, all derivatives are meant as partial ones, indicated by the notation hinting on the convention to insert the x -dependence of \tilde{x} only after differentiating. Inserting this result into the second derivative of Γ_{OM} yields

$$\begin{aligned}
& \frac{\delta^2}{\delta x(t) \delta x(t')} \Gamma_{\text{OM}} [x] \\
&= \frac{\delta}{\delta x(t)} \left[\frac{\delta}{\delta x(t')} \Gamma_{\text{MSRDJ}} [x, \tilde{x}] \Big|_{\tilde{x}=\tilde{x}[x]} + \int ds \frac{\delta}{\delta \tilde{x}(s)} \Gamma_{\text{MSRDJ}} [x, \tilde{x}] \Big|_{\tilde{x}=\tilde{x}[x]} \frac{\delta \tilde{x}(s)}{\delta x(t')} [x] \right] \\
&= \underbrace{\frac{\delta^2}{\delta x(t) \delta x(t')} \Gamma_{\text{MSRDJ}} [x, \tilde{x}] \Big|_{\tilde{x}=\tilde{x}[x]}}_{=\Gamma_{xx}^{(2)}=0} + \int ds \frac{\delta^2}{\delta \tilde{x}(s) \delta x(t')} \Gamma_{\text{MSRDJ}} [x, \tilde{x}] \Big|_{\tilde{x}=\tilde{x}[x]} \frac{\delta \tilde{x}(s)}{\delta x(t)} [x] \\
&+ \underbrace{\int ds \left(\frac{\delta^2 \Gamma_{\text{MSRDJ}} [x, \tilde{x}] \Big|_{\tilde{x}=\tilde{x}[x]}}{\delta x(t) \delta \tilde{x}(s)} \frac{\delta \tilde{x}(s)}{\delta x(t')} [x] + \int ds' \frac{\delta^2 \Gamma_{\text{MSRDJ}} [x, \tilde{x}] \Big|_{\tilde{x}=\tilde{x}[x]}}{\delta \tilde{x}(s) \delta \tilde{x}(s')} \frac{\delta \tilde{x}(s)}{\delta x(t')} [x] \frac{\delta \tilde{x}(s')}{\delta x(t)} [x] \right)}_{\stackrel{(54)}{=}0} \\
&+ \underbrace{\frac{\delta}{\delta \tilde{x}} \Gamma_{\text{MSRDJ}} [x, \tilde{x}] \Big|_{\tilde{x}=\tilde{x}[x]} \frac{\delta^2 \tilde{x}}{\delta x^2} [x]}_{=\Gamma_{\tilde{x}}^{(1)}=0} \\
\stackrel{(55)}{=} & - \int ds \int ds' \left\{ \frac{\delta^2}{\delta x(t') \delta \tilde{x}(s)} \Gamma_{\text{MSRDJ}} [x, \tilde{x}] \Big|_{\tilde{x}=\tilde{x}[x]} \left[\frac{\delta^2}{\delta \tilde{x} \delta \tilde{x}} \Gamma_{\text{MSRDJ}} [x, \tilde{x}] \Big|_{\tilde{x}=\tilde{x}[x]} \right]_{ss'}^{-1} \right. \\
& \quad \left. \times \frac{\delta^2}{\delta \tilde{x}(s') \delta x(t)} \Gamma_{\text{MSRDJ}} [x, \tilde{x}] \Big|_{\tilde{x}=\tilde{x}[x]} \right\} \tag{56} \\
&= \left[\frac{\delta^2}{\delta j(t) \delta j(t')} W [j, \tilde{j}] \right]^{-1} . \tag{57}
\end{aligned}$$

So, expressed in words, the second derivative of Γ_{OM} at x^* equals the inverse of $\langle \delta x \delta x \rangle$. Note that all $[\cdot]^{-1}$ are meant as the inverse of operators acting on functions. For our model, in frequency domain these inversions are simple (matrix) inversions, whereas in time domain this amounts to finding the Green's function of the operator or, in other words, solving a differential equation. Therefore, we can relate the integrated covariances, given by the zero mode of the covariances in Fourier space by Fourier-transforming (57) and inverting it:

$$\frac{\delta^2}{\delta J(\omega)^2} W[J, \tilde{J}] = \left[\frac{\delta^2}{\delta X(\omega)^2} \Gamma_{\text{OM}}[X] \right]^{-1} \quad (58)$$

E. Relation between S_{OM} and S_{MSRDJ} in case of non-Gaussian noise

In this section, we demonstrate that approximations of Γ_{OM} and Γ_{MSRDJ} are not as simply related as their exact counterparts. For non-Gaussian noise, even the comparison of the tree-level-approximations of the effective actions in both formalisms yields counterintuitive results, for example

$$-S_{\text{OM}}[x] \neq \sup_{\tilde{x}} -S_{\text{MSRDJ}}[x, \tilde{x}] \text{ in general,} \quad (59)$$

so even in tree level the equality, which holds for the respective full effective actions, is violated. To see this, consider the SDE:

$$\frac{d}{dt}x = f(x) + \xi,$$

with the cumulant generating function of the noise ξ given by

$$W_{\xi}(y) = \frac{D}{2}y^2 + \frac{\alpha}{3!}y^3$$

and we assume that $\frac{\alpha}{D^2} \ll 1$. The MSRDJ-action is given by

$$S_{\text{MSRDJ}}[x, \tilde{x}] = \tilde{x}(\dot{x} - f(x)) + W_{\xi}(\tilde{x}).$$

We want to calculate

$$S_{\text{OM}} := \ln \left(\int d\tilde{x} \exp(S_{\text{MSRDJ}}[x, \tilde{x}]) \right)$$

to linear order in α . We expand S_{MSRDJ} around the saddle point $\tilde{x}_0[x]$, defined by

$$\frac{\partial S_{\text{MSRDJ}}}{\partial \tilde{x}}[x, \tilde{x}_0[x]] = 0.$$

By expanding $\tilde{x}_0[x]$ in α and inserting it into S and $\frac{\partial^2 S}{\partial \tilde{x}^2}$, we observe that

$$\begin{aligned} S_{\text{MSRDJ}}[x, \tilde{x}_0[x]] &= -\frac{(\dot{x} - f(x))^2}{2D} + \frac{\alpha}{3!} \frac{(f(x) - \dot{x})^3}{D^3} \\ \frac{\partial^2 S_{\text{MSRDJ}}}{\partial \tilde{x}^2}[x, \tilde{x}_0[x]] &= D \left(1 - \frac{\alpha}{D^2} (\dot{x} - f(x)) \right) + \mathcal{O}(\alpha^2). \end{aligned} \quad (60)$$

Computing the contribution from the fluctuations around the stationary point with respect to \tilde{x} yields

$$\begin{aligned} & \int d\tilde{x} \exp(S_{\text{MSRDJ}}[x, \tilde{x}]) \\ &= \int d\tilde{x} \exp \left(S_{\text{MSRDJ}}[x, \tilde{x}_0] + \frac{\partial^2 S_{\text{MSRDJ}}}{\partial \tilde{x}^2}[x, \tilde{x}_0] \frac{(\tilde{x} - \tilde{x}_0[x])^2}{2} + \underbrace{\frac{\partial^3 S_{\text{MSRDJ}}}{\partial \tilde{x}^3}[x, \tilde{x}_0]}_{=\alpha} \frac{(\tilde{x} - \tilde{x}_0[x])^3}{3!} \right) \\ & \stackrel{y = (\tilde{x} - \tilde{x}_0[x])}{=} \exp(S_{\text{MSRDJ}}[x, \tilde{x}_0[x]]) \int dy \exp \left(\frac{1}{2} \frac{\partial^2 S_{\text{MSRDJ}}}{\partial \tilde{x}^2}[x, \tilde{x}_0] y^2 \right) \left(1 + \frac{1}{3!} \alpha y^3 \right) + \mathcal{O}(\alpha^2) \\ &= \exp(S_{\text{MSRDJ}}[x, \tilde{x}_0[x]]) \sqrt{\frac{2\pi}{\frac{\partial^2 S_{\text{MSRDJ}}}{\partial \tilde{x}^2}[x, \tilde{x}_0]}} + \mathcal{O}(\alpha^2) \\ &= \exp(S_{\text{MSRDJ}}[x, \tilde{x}_0[x]]) \sqrt{\frac{2\pi}{D \left(1 - \frac{\alpha}{D^2} (\dot{x} - f(x)) \right)}} + \mathcal{O}(\alpha^2) \\ &= \exp \left(-\frac{(\dot{x} - f(x))^2}{2D} + \frac{\alpha}{3!} \frac{(f(x) - \dot{x})^3}{D^3} \right) \sqrt{\frac{2\pi}{D}} \left(1 + \frac{\alpha}{2D^2} (\dot{x} - f(x)) \right) + \mathcal{O}(\alpha^2). \end{aligned}$$

So, in total, we have

$$S_{\text{OM}}[x] = \frac{1}{2} \ln \left(\frac{2\pi}{D} \right) - \frac{(\dot{x} - f(x))^2}{2D} - \frac{\alpha}{3!} \frac{(\dot{x} - f(x))^3}{D^3} + \frac{\alpha}{2D^2} (\dot{x} - f(x)) + \mathcal{O}(\alpha^2).$$

So the fluctuations around the saddle-point value of the action lead to additional terms contributing to S_{OM} , not only constant, but also x -dependent ones. We can reformulate this to (59), so the relation we obtained for the respective effective actions does not hold for the actions, i.e. the tree-level approximations of the effective actions.

F. Graphical derivation for the small parameter of the loop expansion

In this chapter, we convince ourselves that introducing an extra loop in a diagram leads to a contribution of order $D\beta^2$ times the order of the diagram we start with. Adding a loop means attaching a propagator-line to two points in the original diagram. This requires points at which exactly three lines meet; if we had interactions higher than three, there

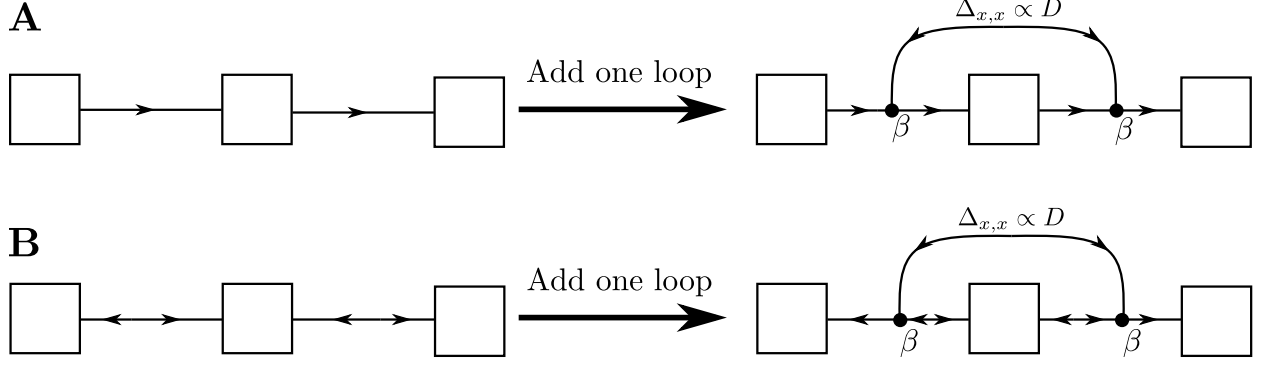


Figure 6. Adding an additional loop to an arbitrary diagram: In (A), we attach the concerning line to two $\Delta_{x\tilde{x}}$ -lines, in (B) to two Δ_{xx} -lines. The mixed case is analogous and therefore omitted.

could also be more. The interaction bears the strength β which leads to the part β^2 in the loop expansion-parameter. It is not clear a priori, however, that the line connecting these two interactions cannot be a $\Delta_{\tilde{x}\tilde{x}}$ -line. But Figure 6 demonstrates that the form of the interaction with two ingoing lines and one outgoing line always forces us to plug in an undirected line or, in another words, a Δ_{xx} -propagator, which introduces the factor D .

G. One-loop result of the propagator

We obtain the one-loop approximation of the propagator by solving $\Gamma^{(2)}\Delta = \left(-S^{(2)} + \Gamma_{\text{fl.}}^{(2)}\right)\Delta = 1$ for Δ . In frequency domain this yields

$$1 = \begin{pmatrix} \Gamma_{X\tilde{X}}^{(2)}(\omega) \Delta_{\tilde{X}X}(-\omega) & \Gamma_{X\tilde{X}}^{(2)}(\omega) \Delta_{\tilde{X}\tilde{X}}(-\omega) \\ \Gamma_{\tilde{X}X}^{(2)}(\omega) \Delta_{XX}(-\omega) - \Gamma_{\tilde{X}\tilde{X}}^{(2)}(\omega) \Delta_{\tilde{X}X}(-\omega) & \Gamma_{\tilde{X}X}^{(2)}(\omega) \Delta_{X\tilde{X}}(-\omega) - \Gamma_{\tilde{X}\tilde{X}}^{(2)}(\omega) \Delta_{\tilde{X}\tilde{X}}(-\omega) \end{pmatrix}, \quad (61)$$

where

$$\Gamma^{(2)}(\omega) = \begin{pmatrix} 0 & \left(-i\omega + m + \frac{A}{-i\omega + 2m}\right) \\ \left(i\omega + m + \frac{A}{i\omega + 2m}\right) & D \left(1 - \frac{A}{\omega^2 + (2m)^2}\right) \end{pmatrix}.$$

Equation (61) is solved by

$$\begin{aligned} \Delta_{\tilde{X}\tilde{X}}(\omega) &= 0 \\ \Delta_{\tilde{X}X}(\omega) &= [\Delta_{X\tilde{X}}(\omega)]^* = \frac{i\omega + 2m}{(i\omega + m)(i\omega + 2m) + A} \\ \Delta_{XX}(\omega) &= \Delta_{x\tilde{x}}(\omega) D \Delta_{\tilde{x}x}(\omega) - \Delta_{x\tilde{x}}(\omega) \Gamma_{\tilde{X}X,\text{fl.}}^{(2)}(\omega) D A \Gamma_{X\tilde{X},\text{fl.}}^{(2)}(\omega) \Delta_{\tilde{x}x}(\omega), \end{aligned}$$

where $A = 2\beta^2 D/m$. Moreover, we introduced the notation $\Delta(\omega, \omega') = \Delta(\omega) 2\pi\delta(\omega + \omega')$.

In time domain these equations read

$$\begin{aligned}\Delta_{\tilde{x}x}(t, t') &= \Delta_{x\tilde{x}}(t', t) = -H(t' - t) \left[\frac{m_1 - 2m}{m_1 - m_2} e^{m_1|t-t'|} + \frac{2m - m_2}{m_1 - m_2} e^{m_2|t-t'|} \right] \\ \Delta_{xx}(t', t) &= - \left[\frac{D(m_1^2 - (2m)^2 + A)}{2(m_1^2 - m_2^2)m_1} e^{m_1|t-t'|} + \frac{D((2m)^2 - m_2^2 - A)}{2(m_1^2 - m_2^2)m_2} e^{m_2|t-t'|} \right],\end{aligned}$$

where $m_{1/2} = 3m/2 \pm \sqrt{m^2/4 - A}$ for which the relation $m_2 < 2m < m < m_1 < 0$ holds in case of a choice of parameters for which the classical fixed point x_0 is stable.

H. Three-point interaction vertex in time domain

In time domain the one-loop approximation of the three-point interaction vertex is given by

$$\Gamma_{\tilde{x}xx, \text{fl.}}^{(3)}(t_1, t_2, t_3) = \begin{cases} -8\beta^3 \frac{D}{m} e^{2m(t_1-t_3)} & , t_1 > t_2 > t_3 \\ -8\beta^3 \frac{D}{m} e^{2m(t_1-t_2)} & , t_1 > t_3 > t_2 \\ 0 & , \text{else} \end{cases}$$

For the BMW approximation we will need the two quantities $\Gamma_{\tilde{X}XX, \text{fl.}}^{(3)}(\sigma_1, -\sigma_1, 0)$ and $\Gamma_{\tilde{X}XX, \text{fl.}}^{(3)}(0, \sigma_2, -\sigma_2)$ which in one-loop approximation read

$$\begin{aligned}\Gamma_{\tilde{X}XX, \text{fl.}}^{(3)}(\sigma_1, -\sigma_1, 0) &= -\frac{4\beta^3 D}{(2\pi)^2} \frac{4m + i\sigma_1}{m^2 (2m + i\sigma_1)^2} \\ \Gamma_{\tilde{X}XX, \text{fl.}}^{(3)}(0, \sigma_2, -\sigma_2) &= -\frac{16\beta^3 D}{(2\pi)^2} \frac{1}{m \sigma_2^2 + 4m^2},\end{aligned}$$

which in time domain yields

$$\begin{aligned}\Gamma_{\tilde{x}xx, \text{fl.,1}}^{(3)}(t_1, t_2) &= -\frac{8\beta^3 D}{2\pi m} H(t_1 - t_2) \left(t_1 - t_2 - \frac{1}{2m} \right) e^{2m(t_1-t_2)} \\ \Gamma_{\tilde{x}xx, \text{fl.,2}}^{(3)}(t_1, t_2) &= \frac{8\beta^3 D}{2\pi m} \frac{1}{2m} e^{2m|t_1-t_2|}.\end{aligned}$$

I. Equation of motion for δx from Fokker-Plank equation

We start by multiplying the Fokker-Plank equation [58] for a time-dependent density

$$\tau \partial_t \rho(x, t) = -\partial_x \left(f(x) - \frac{D}{2} \partial_x \right) \rho(x, t)$$

by x and integrating over x :

$$\begin{aligned}\partial_t \langle x \rangle (t) &= - \int dx x \left(\partial_x (f(x) \rho(x, t)) - \frac{D}{2} \partial_x^2 \rho(x, t) \right) \\ &= \int dx f(x) \rho(x, t) = -l \langle x(t) \rangle + \beta \langle x(t)^2 \rangle,\end{aligned}$$

where from the first to the second line we used partial integration. From the second term only a derivative under an integral remains, which vanishes because we assume that ρ vanishes at the borders of the integral - a property that we will use repeatedly in the following. In the last equality, furthermore, we inserted $f(x) = -lx + \beta x^2$. Now, we need an ODE for the second moment, which we obtain analogously:

$$\begin{aligned}\partial_t \langle x^2 \rangle (t) &= - \int dx x^2 \left(\partial_x (f(x) \rho(x, t)) - \frac{D}{2} \partial_x^2 \rho(x, t) \right) \\ &= \int dx (2xf(x) \rho(x, t) - Dx \partial_x \rho(x, t)) \\ &= \int dx (2xf(x) \rho(x, t) + D\rho(x, t)) \\ &= -2l \langle x^2 \rangle (t) + 2\beta \langle x^3 \rangle (t) + D.\end{aligned}$$

Truncating the hierarchy of moments by a Gaussian closure, that is

$$\begin{aligned}\langle x^3 \rangle &= \langle\langle x^3 \rangle\rangle + 3\langle\langle x^2 \rangle\rangle \langle\langle x \rangle\rangle + \langle\langle x \rangle\rangle^3 \\ &= \langle\langle x^3 \rangle\rangle + 3\langle x^2 \rangle \langle x \rangle - 2\langle x \rangle^3 \approx 3\langle x^2 \rangle \langle x \rangle - 2\langle x \rangle^3\end{aligned}$$

leads to

$$\partial \langle x^2 \rangle (t) \approx -2l \langle x^2 \rangle (t) + 6\beta \langle x^2 \rangle (t) \langle x \rangle (t) - 4\beta (\langle x \rangle (t))^3 + D.$$

Using $\langle\langle x^2 \rangle\rangle = \langle x^2 \rangle - \langle x \rangle^2$, the equations for the first two cumulants read:

$$\partial_t \langle\langle x \rangle\rangle (t) = -l \langle\langle x \rangle\rangle (t) + \beta (\langle\langle x^2 \rangle\rangle (t) + (\langle\langle x \rangle\rangle (t))^2) \quad (62)$$

$$\partial_t \langle\langle x^2 \rangle\rangle (t) = -2l \langle\langle x^2 \rangle\rangle (t) + 4\beta \langle\langle x^2 \rangle\rangle (t) \langle\langle x \rangle\rangle (t) + D \quad (63)$$

We can interpret the one-loop equation of motion as an approximation of the solution of the Fokker-Planck equations of motion (62) and (63). To see this, we formally solve (63) and insert the result into (62). It is convenient to express the time dependence of x and Δ as a deviation from the stationary solution, defining

$$\langle x \rangle (t) = \bar{x} + \delta x (t) \quad (64)$$

$$\langle\langle x^2 \rangle\rangle (t) = \bar{\Delta} + \delta \Delta (t) \quad (65)$$

$$\bar{m} = -l + 2\beta \bar{x}$$

$$m(t) = -l + 2\beta \langle x \rangle (t) = \bar{m} + 2\beta \delta x (t).$$

Using these definitions, for the stationary case

$$0 = -l\bar{x} + \beta\bar{x}^2 + \beta\bar{\Delta} \quad \text{and} \quad \bar{\Delta} = -\frac{D}{2\bar{m}},$$

which follows from (62) and (63), respectively. Expressing these equations in the new variables (64) and (65) yields

$$\begin{aligned} \partial_t \delta x(t) &= \partial_t \langle\langle x \rangle\rangle(t) = -(l - 2\beta\bar{x})\delta x(t) + \beta\delta x(t)^2 \underbrace{-l\bar{x} + \beta\bar{x}^2 + \beta\bar{\Delta}}_{=0} + \beta\delta\Delta(t) \\ &= \bar{m}\delta x(t) + \beta\delta x(t)^2 + \beta\delta\Delta(t) \end{aligned} \quad (66)$$

and

$$\begin{aligned} \partial_t \delta\Delta(t) &= \underbrace{2\bar{m}\bar{\Delta} + D}_{=0} + 2(\bar{m} + 2\beta\delta x(t))\delta\Delta(t) + 4\beta\bar{\Delta}\delta x(t) \\ &= 2m(t)\delta\Delta(t) + 4\beta\bar{\Delta}\delta x(t). \end{aligned}$$

The latter equation turns out to be more convenient for our purpose compared to (63). Solving it by variation of constants, we obtain

$$\begin{aligned} \delta\Delta(t) &= 4\beta\bar{\Delta} \int_{t_0}^t dt'' \delta x(t'') e^{\int_{t''}^t dt' 2m(t')} \\ &= 4\beta\bar{\Delta} \int_{t_0}^t dt'' \delta x(t'') e^{2\bar{m}(t-t'')} e^{4\beta \int_{t''}^t dt' \delta x(t')}, \end{aligned} \quad (67)$$

where we introduced the initial time t_0 . We notice that $\langle\langle x^2 \rangle\rangle(t = t_0) = \Delta^*$, since $\delta\Delta(t = t_0) = 0$, which corresponds to distributing according to the stationary distribution with mean value shifted by the initial deflection $\delta x(t_0)$. If we assume that $\delta x(t)$ is small for all t , we can expand the second exponential function in (67) and neglect terms of $\mathcal{O}(\delta x^3)$. Thus

$$\begin{aligned} \delta\Delta(t) &= 4\beta\bar{\Delta} \int_{t_0}^t dt'' \delta x(t'') e^{2\bar{m}(t-t'')} + 16\bar{\Delta}\beta^2 \int_{t_0}^t dt'' \delta x(t'') e^{2\bar{m}(t-t'')} \int_{t''}^t dt' \delta x(t') + \mathcal{O}(\delta x^3) \\ &= 4\beta\bar{\Delta} \int_{t_0}^t dt' \delta x(t') e^{2\bar{m}(t-t')} + 16\bar{\Delta}\beta^2 \int_{t_0}^t dt' \delta x(t') \int_{t_0}^{t'} dt'' \delta x(t'') e^{2\bar{m}(t-t'')} + \mathcal{O}(\delta x^3). \end{aligned}$$

If we insert this result into (66) we obtain up to second order

$$\begin{aligned} \partial_t \delta x(t) &= \bar{m}\delta x(t) + \beta\delta x(t)^2 \\ &\quad + 4\beta^2\bar{\Delta} \int_{t_0}^t dt' \delta x(t') e^{2\bar{m}(t-t')} \\ &\quad + 16\bar{\Delta}\beta^3 \int_{t_0}^t dt' \delta x(t') \int_{t_0}^{t'} dt'' \delta x(t'') e^{2\bar{m}(t-t'')}, \end{aligned}$$

which equals exactly the one-loop result (34).

J. Derivation of fRG-flow equations

For completeness, the derivation of the Wetterich equation [35] as presented in [36] is repeated in the following. The difference of the current presentation is the additional presence of the response field. We will use the property $\partial_\lambda \Gamma_\lambda = -\partial_\lambda W_\lambda$, which holds generally for Legendre transforms of quantities depending on a parameter, here λ [4, eq. (1.93)]. This yields, using the regulator of the form introduced in (38),

$$\begin{aligned}
& \frac{\partial \tilde{\Gamma}_\lambda[X^*, \tilde{X}^*]}{\partial \lambda} = -\frac{\partial W_\lambda[J, \tilde{J}]}{\partial \lambda} \\
& = -\frac{1}{\mathcal{Z}[J, \tilde{J}]} \int \mathcal{D}X \int \mathcal{D}\tilde{X} \frac{\partial}{\partial \lambda} \Delta S_\lambda[X, \tilde{X}] \exp(S_\lambda[X, \tilde{X}]) \\
& \quad \times \exp(J^\text{T} X + \tilde{J}^\text{T} \tilde{X}) \\
& = \frac{1}{2} \int d\omega \int d\omega' \langle X(\omega) \frac{\partial R_\lambda(\omega, \omega')}{\partial \lambda} \tilde{X}(\omega') \rangle \\
& = \frac{1}{2} \int d\omega \int d\omega' \left\{ \Delta_{\tilde{X}X, \lambda}(\omega', \omega) \frac{\partial R_\lambda(\omega, \omega')}{\partial \lambda} + X^*(\omega) \frac{\partial R_\lambda(\omega, \omega')}{\partial \lambda} \tilde{X}^*(\omega') \right\} \\
& = \frac{1}{2} \text{Tr} \left\{ \Delta_{\tilde{X}X, \lambda} \frac{\partial R_\lambda}{\partial \lambda} \right\} + \frac{\partial}{\partial \lambda} \Delta S_\lambda[X^*, \tilde{X}^*]. \tag{68}
\end{aligned}$$

In the third line we used $\langle \tilde{X}(\omega') X(\omega) \rangle = \langle \langle \tilde{X}(\omega) X(\omega') \rangle \rangle + \langle \tilde{X}(\omega') \rangle \langle X(\omega) \rangle = \Delta_{\tilde{X}X, \lambda}(\omega', \omega) + X^*(\omega) \tilde{X}^*(\omega')$. Because of the definition of Γ_λ , in its derivative with respect to λ , the last term of (68) is removed.

K. Flow equations for the self-energy and the interaction vertex

The non-vanishing diagrams for the self-energy translate to

$$\begin{aligned}
\frac{\partial \Gamma_{\tilde{X}X,\lambda}^{(2)}(\sigma_1, -\sigma_1)}{\partial \lambda} &= \frac{1}{2} \int \frac{d\omega}{(2\pi)} \Gamma_{\tilde{X}XX,\lambda}^{(3)}(\sigma_1, -\sigma_1 - \omega, \omega) \Delta_{XX,\lambda}(\omega) \frac{\partial R_\lambda}{\partial \lambda} \Delta_{\tilde{X}X,\lambda}(\omega) \\
&\quad \times \Gamma_{XX\tilde{X},\lambda}^{(3)}(-\sigma_1, -\omega, \sigma_1 + \omega) \Delta_{\tilde{X}X,\lambda}(\sigma_1 + \omega) \\
&+ \frac{1}{2} \int \frac{d\omega}{(2\pi)} \Gamma_{\tilde{X}XX,\lambda}^{(3)}(\sigma_1, -\sigma_1 - \omega, \omega) \Delta_{XX,\lambda}(\omega) \Gamma_{XX\tilde{X},\lambda}^{(3)}(-\sigma_1, -\omega, \sigma_1 + \omega) \\
&\quad \times \Delta_{\tilde{X}X,\lambda}(\sigma_1 + \omega) \frac{\partial R_\lambda}{\partial \lambda} \Delta_{\tilde{X}X,\lambda}(\sigma_1 + \omega) \\
&+ \frac{1}{2} \int \frac{d\omega}{(2\pi)} \Gamma_{\tilde{X}XX,\lambda}^{(3)}(\sigma_1, -\sigma_1 - \omega, \omega) \Delta_{X\tilde{X},\lambda}(\omega) \Gamma_{X\tilde{X},\lambda}^{(3)}(-\sigma_1, -\omega, \sigma_1 + \omega) \\
&\quad \times \Delta_{XX,\lambda}(\sigma_1 + \omega) \frac{\partial R_\lambda}{\partial \lambda} \Delta_{\tilde{X}X,\lambda}(\sigma_1 + \omega) \\
\frac{\partial \Gamma_{\tilde{X}\tilde{X},\lambda}^{(2)}(\sigma_1, -\sigma_1)}{\partial \lambda} &= \frac{1}{2} \int \frac{d\omega}{(2\pi)} \Gamma_{\tilde{X}XX,\lambda}^{(3)}(\sigma_1, -\sigma_1 - \omega, \omega) \Delta_{XX,\lambda}(\omega) \frac{\partial R_\lambda}{\partial \lambda} \Delta_{\tilde{X}X,\lambda}(\omega) \\
&\quad \times \Gamma_{\tilde{X}XX,\lambda}^{(3)}(-\sigma_1, -\omega, \sigma_1 + \omega) \Delta_{XX,\lambda}(\sigma_1 + \omega) \\
&+ \sigma_1 \rightarrow -\sigma_1.
\end{aligned}$$

The diagrams for the flow of the interaction vertex are given by

$$\begin{aligned}
 & \frac{\partial \Gamma_{\tilde{X}X\lambda}^{(3)}(\sigma_1, \sigma_2, \sigma_3)}{\partial \lambda} \\
 &= -\frac{1}{2} \left[\begin{array}{c} \text{Diagram 1: Circle with vertices } \sigma_1, \sigma_2, \sigma_3. \text{ Wavy lines at } \sigma_1, \sigma_2, \sigma_3. \text{ Square on } \sigma_2 \rightarrow \sigma_3 \text{ arc.} \\ \text{Diagram 2: Circle with vertices } \sigma_1, \sigma_2, \sigma_3. \text{ Wavy lines at } \sigma_1, \sigma_2, \sigma_3. \text{ Square on } \sigma_1 \rightarrow \sigma_2 \text{ arc.}} \\ + \\ \begin{array}{c} \text{Diagram 3: Circle with vertices } \sigma_1, \sigma_2, \sigma_3. \text{ Wavy lines at } \sigma_1, \sigma_2, \sigma_3. \text{ Square on } \sigma_3 \rightarrow \sigma_1 \text{ arc.} \\ \text{Diagram 4: Circle with vertices } \sigma_1, \sigma_2, \sigma_3. \text{ Wavy lines at } \sigma_1, \sigma_2, \sigma_3. \text{ Square on } \sigma_2 \rightarrow \sigma_1 \text{ arc.} \\ \text{Diagram 5: Circle with vertices } \sigma_1, \sigma_2, \sigma_3. \text{ Wavy lines at } \sigma_1, \sigma_2, \sigma_3. \text{ Square on } \sigma_1 \rightarrow \sigma_3 \text{ arc.} \\ \text{Diagram 6: Circle with vertices } \sigma_1, \sigma_2, \sigma_3. \text{ Wavy lines at } \sigma_1, \sigma_2, \sigma_3. \text{ Square on } \sigma_3 \rightarrow \sigma_2 \text{ arc.} \end{array} \right] \\
 &+ \sigma_2 \leftrightarrow \sigma_3.
 \end{aligned}$$

L. Definition of the Fourier transform

By choosing the Fourier transform of the fields and the sources as the inverse of each other, we arrive at a representation of our formulas that look similar in time and frequency domain. Therefore we define

$$\begin{aligned}
 x(t) &= \int \frac{d\omega}{2\pi} e^{i\omega t} X(\omega) & j(t) &= \int d\omega e^{-i\omega t} J(\omega) \\
 X(\omega) &= \int dt e^{-i\omega t} x(t) & J(\omega) &= \int \frac{dt}{2\pi} e^{i\omega t} j(t).
 \end{aligned}$$

Thus, we obtain $x^T j = \int dt x(t) j(t) = \int d\omega X(\omega) J(\omega)$. Moreover, we get with $y := (x, \tilde{x})^T$ for the matrix A of the quadratic part of the action $S_0[x, \tilde{x}] = \int dt \int dt' y(t) A(t, t') y(t')$

$$\begin{aligned} A(t, t') &= \int d\omega \int d\omega' e^{-i(\omega t + \omega' t')} A(\omega, \omega') & A^{-1}(t, t') &= \int \frac{d\omega}{2\pi} \int \frac{d\omega'}{2\pi} e^{i(\omega t + \omega' t')} A^{-1}(\omega, \omega') \\ A(\omega, \omega') &= \int \frac{dt}{2\pi} \int \frac{dt'}{2\pi} e^{i(\omega t + \omega' t')} A(t, t') & A^{-1}(\omega, \omega') &= \int dt \int dt' e^{-i(\omega t + \omega' t')} A^{-1}(t, t') \end{aligned}$$

due to the chain rule for functional derivatives. From this we can derive the following useful identities

$$\begin{aligned} \int dt \int dt' y(t) A(t, t') y(t') &= \int d\omega \int d\omega' Y(\omega) A(\omega, \omega') Y(\omega') \\ \int dt \int dt' \bar{j}(t) A^{-1}(t, t') \bar{j}(t') &= \int d\omega \int d\omega' \bar{J}(\omega) A^{-1}(\omega, \omega') \bar{J}(\omega') \end{aligned}$$

$$\int ds A(t, s) A^{-1}(s, t') = \delta(t - t') \quad \Leftrightarrow \quad \int d\sigma A(\omega, \sigma) A^{-1}(\sigma, \omega') = \delta(\omega - \omega').$$

For the interaction part of the action we obtain

$$\int dt \tilde{x}(t) x^2(t) = \int \frac{d\omega}{2\pi} \int \frac{d\omega'}{2\pi} \tilde{X}(\omega) X(\omega') X(-\omega - \omega').$$

-
- [1] D. Dahmen, H. Bos, and M. Helias, *Phys. Rev. X* **6**, 031024 (2016).
 - [2] H. Sompolinsky, *Physics Today* **70**, 80 (1988).
 - [3] V. Braitenberg and A. Schüz, *Anatomy of the Cortex: Statistics and Geometry* (Springer-Verlag, Berlin, Heidelberg, New York, 1991), ISBN 3-540-53233-1.
 - [4] J. Zinn-Justin, *Quantum field theory and critical phenomena* (Clarendon Press, Oxford, 1996).
 - [5] P. C. Hohenberg and B. I. Halperin, *Rev. Mod. Phys.* **49**, 435 (1977).
 - [6] U. C. Täuber, *Critical dynamics: a field theory approach to equilibrium and non-equilibrium scaling behavior* (Cambridge University Press, 2014), ISBN 9780521842235.
 - [7] C. Chow and M. Buice, *The Journal of Mathematical Neuroscience* **5** (2015).
 - [8] J. A. Hertz, Y. Roudi, and P. Sollich, *Journal of Physics A: Mathematical and Theoretical* **50**, 033001 (2017).
 - [9] C. van Vreeswijk and H. Sompolinsky, *Science* **274**, 1724 (1996).
 - [10] D. J. Amit and N. Brunel, *Network: Comput. Neural Systems* **8**, 373 (1997).

- [11] N. Brunel, *J. Comput. Neurosci.* **8**, 183 (2000).
- [12] J. J. Hopfield, *PNAS* **79**, 2554 (1982).
- [13] M. Schmidt, R. Bakker, C. C. Hilgetag, M. Diesmann, and S. J. van Albada, *Brain Structure and Function* (2017).
- [14] J. Schuecker, M. Schmidt, S. J. van Albada, M. Diesmann, and M. Helias, *PLOS Comput. Biol.* **13**, e1005179 (2017).
- [15] I. Ginzburg and H. Sompolinsky, *Phys. Rev. E* **50**, 3171 (1994).
- [16] A. Renart, J. De La Rocha, P. Bartho, L. Hollender, N. Parga, A. Reyes, and K. D. Harris, *Science* **327**, 587 (2010).
- [17] M. Helias, T. Tetzlaff, and M. Diesmann, *PLOS Comput. Biol.* **10**, e1003428 (2014).
- [18] E. Shea-Brown, K. Josic, J. de la Rocha, and B. Doiron, *Phys. Rev. Lett.* **100**, 108102 (2008).
- [19] V. Pernice, B. Staude, S. Cardanobile, and S. Rotter, *PLOS Comput. Biol.* **7**, e1002059 (2011).
- [20] V. Pernice, B. Staude, S. Cardanobile, and S. Rotter, *Phys. Rev. E* **85**, 031916 (2012).
- [21] T. Tetzlaff, M. Helias, G. T. Einevoll, and M. Diesmann, *PLOS Comput. Biol.* **8**, e1002596 (2012).
- [22] J. Trousdale, Y. Hu, E. Shea-Brown, and K. Josic, *PLOS Comput. Biol.* **8**, e1002408 (2012).
- [23] Y. Hu, J. Trousdale, K. Josić, and E. Shea-Brown, *Journal of Statistical Mechanics: Theory and Experiment* **2013**, P03012 (2013).
- [24] N. Brunel and V. Hakim, *Neural Comput.* **11**, 1621 (1999).
- [25] N. Brunel, *J. Comput. Neurosci.* **8**, 183 (2000).
- [26] M. Helias, T. Tetzlaff, and M. Diesmann, *New J. Phys.* **15**, 023002 (2013).
- [27] H. Bos, M. Diesmann, and M. Helias, *PLOS Comput. Biol.* **12**, e1005132 (2016).
- [28] J. M. Beggs and D. Plenz, *J. Neurosci.* **24**, 5216 (2004).
- [29] G. Tkačik, O. Marre, D. Amodei, E. Schneidman, W. Bialek, and M. J. Berry II, *PLoS Comp Biol* **10**, e1003408 (2014).
- [30] H. Jaeger, *Tech. Rep. GMD Report 148*, German National Research Center for Information Technology, St. Augustin, Germany (2001).
- [31] W. Maass, T. Natschläger, and H. Markram, *Neural Comput.* **14**, 2531 (2002).
- [32] R. Legenstein and W. Maass, *Neural Networks* **20**, 323 (2007).
- [33] K. G. Wilson, *Rev. Mod. Phys.* **47**, 773 (1975).

- [34] F. J. Wegner and A. Houghton, Phys. Rev. A **8**, 401 (1973).
- [35] C. Wetterich, Physics Letters B **301**, 90 (1993), ISSN 0370-2693.
- [36] J. Berges, N. Tetradis, and C. Wetterich, Physics Reports **363**, 223 (2002), ISSN 0370-1573, renormalization group theory in the new millennium. {IV}.
- [37] P. Martin, E. Siggia, and H. Rose, Phys. Rev. A **8**, 423 (1973).
- [38] H.-K. Janssen, Zeitschrift für Physik B Condensed Matter **23**, 377 (1976).
- [39] C. De Dominicis, J. Phys. Colloques **37**, C1 (1976).
- [40] H. Sompolinsky and A. Zippelius, Phys. Rev. Lett. **47**, 359 (1981).
- [41] K. Fischer and J. Hertz, *Spin glasses* (Cambridge University Press, 1991).
- [42] A. Crisanti and H. Sompolinsky, Phys. Rev. E **98**, 062120 (2018).
- [43] J. Schuecker, S. Goedeke, and M. Helias, Phys. Rev. X **8**, 041029 (2018).
- [44] S. Song, P. Sjöström, M. Reigl, S. Nelson, and D. Chklovskii, PLoS Biol. **3**, e68 (2005).
- [45] D. Martí, N. Brunel, and S. Ostoic, Phys. Rev. E **97**, 062314 (2018).
- [46] C. Gardiner, *Stochastic Methods: A Handbook for the Natural and Social Sciences* (Springer, Berlin, Heidelberg, 2009), 4th ed.
- [47] N. G. Van Kampen, *Stochastic Processes in Physics and Chemistry, Third Edition (North-Holland Personal Library)* (North Holland, 2007), 3rd ed.
- [48] H. Kleinert, *Path Integrals in Quantum Mechanics, Statistics, Polymer Physics, and Financial Markets* (World Scientific, 2009), 5th ed.
- [49] L. Onsager and S. Machlup, **91**, 1505 (1953).
- [50] R. L. Stratonovich, in *Proc. Sixth All-Union Conf. Theory Prob. and Math. Statist, Vilnius* (1960), pp. 471–482, translation to english by A. N. Rossolimo published in "Selected Transl. in Math. Statist. and Probability, Vol. 10, 1971".
- [51] C. W. Gardiner, *Handbook of Stochastic Methods for Physics, Chemistry and the Natural Sciences* (Springer-Verlag, Berlin, 1985), 2nd ed., ISBN 3-540-61634-9, 3-540-15607-0.
- [52] R. Graham, Zeitschrift für Physik B Condensed Matter **26**, 281 (1977), ISSN 1431-584X.
- [53] K. L. C. Hunt and J. Ross, The Journal of Chemical Physics **75**, 976 (1981), <https://doi.org/10.1063/1.442098>.
- [54] Note1, note that the notation as an integral is meant symbolically: For concrete calculations of the path integral, one always has to use the discrete version with a finite sum, perform the integrations and draw the limit afterwards.

- [55] A. C. C. Coolen, arXiv:cond-mat/0006011 (2000).
- [56] H. Sompolinsky and A. Zippelius, Phys. Rev. B **25**, 6860 (1982).
- [57] C. De Dominicis, Phys. Rev. B **18**, 4913 (1978).
- [58] H. Risken, *The Fokker-Planck Equation* (Springer Verlag Berlin Heidelberg, 1996), URL https://doi.org/10.1007/978-3-642-61544-3_4.
- [59] A. Vasiliev, *Functional Methods in Quantum Field Theory and Statistical Physics* (Gordon and Breach Science Publishers, 1998).
- [60] Note2, at least in physically reasonable settings: A discontinuity in the derivative in Φ means that Γ has a discontinuity, too, and therefore W , in turn, would have a flat segment. In such systems, changing the source field would not affect the mean.
- [61] D. J. Amit, *Field theory, the renormalization group, and critical phenomena* (World Scientific, 1984).
- [62] J. W. Negele and H. Orland, *Quantum Many-Particle Systems* (New York: Perseus Books, 1998).
- [63] F. Cooper and J. F. Dawson, arxiv preprint arXiv:1406.2737 (2015).
- [64] M. A. Buice and C. C. Chow, Phys. Rev. E **76**, 031118 (2007).
- [65] J. E. Mayer and M. Goeppert-Mayer, *Statistical mechanics* (John Wiley & Sons, Inc., 1977), 2nd ed.
- [66] A. Roxin, N. Brunel, D. Hansel, G. Mongillo, and C. van Vreeswijk, J. Neurosci. **31**, 16217 (2011).
- [67] L. Ornigotti, A. Ryabov, V. Holubec, and R. Filip, Phys. Rev. E **97**, 032127 (2018).
- [68] R. Filip and P. Zemánek, Journal of Optics **18**, 065401 (2016).
- [69] M. A. Buice and J. D. Cowan, Phys. Rev. E **75**, 051919 (2007).
- [70] M. Doi, Journal of Physics A: Mathematical and General **9**, 1465 (1976).
- [71] L. Peliti, J. Phys. France pp. 1469–1483 (1985).
- [72] R. Zwanzig, *Nonequilibrium Statistical Mechanics* (Oxford University Press, 2001), ISBN 0-19-514018-4.
- [73] B. Bravi, P. Sollich, and M. Opper, Journal of Physics A: Mathematical and Theoretical **49**, 194003 (2016).
- [74] C. De Dominicis and P. C. Martin, Journal of Mathematical Physics **5**, 14 (1964).

- [75] T. R. MORRIS, *International Journal of Modern Physics A* **09**, 2411 (1994), <https://doi.org/10.1142/S0217751X94000972>.
- [76] C. Bagnuls and C. Bervillier, *Physics Reports* **348**, 91 (2001), ISSN 0370-1573, renormalization group theory in the new millennium. II.
- [77] Note3, the condition $\Gamma_{\tilde{x},\lambda}^{(1)}[x_\lambda^*, \tilde{x}_\lambda^*] = 0$ would of course lead to the same result because we are eventually interested in $\lambda = 0$, where both quantities agree, but using $\tilde{\Gamma}$ leads to the occurrence of the propagator including the regulator term in (41), which is more convenient.
- [78] F. Schütz and P. Kopietz, *Journal of Physics A: Mathematical and General* **39**, 8205 (2006).
- [79] P. Kopietz, L. Bartosch, and F. Schütz, *Introduction to the Functional Renormalization Group* (Springer, 2010).
- [80] J.-P. Blaizot, R. Méndez-Galain, and N. Wschebor, *Physics Letters B* **632**, 571 (2006), ISSN 0370-2693.
- [81] J.-P. Blaizot, R. Méndez-Galain, and N. Wschebor, *Phys. Rev. E* **74**, 051116 (2006).
- [82] L. Canet, H. Chaté, B. Delamotte, and N. Wschebor, *Phys. Rev. Lett.* **104**, 150601 (2010).
- [83] F. Benitez, J.-P. Blaizot, H. Chaté, B. Delamotte, R. Méndez-Galain, and N. Wschebor, *Phys. Rev. E* **85**, 026707 (2012).
- [84] S. H. Strogatz, *Nonlinear Dynamics and Chaos: with Applications to Physics, Biology, Chemistry, and Engineering* (Perseus Books, Reading, Massachusetts, 1994), ISBN 0-201-54344-3.
- [85] G. Buzsáki and A. Draguhn, *Science* **304**, 1926 (2004).
- [86] N. Brunel and X.-J. Wang, *J. Neurophysiol.* **90**, 415 (2003).
- [87] K. Takahashi, S. Kim, T. P. Coleman, K. A. Brown, A. J. Suminski, M. D. Best, and N. G. Hatsopoulos, *Nature Communications* **6** (2015).
- [88] M. Denker, L. Zehl, B. E. Kilavik, M. Diesmann, T. Brochier, A. Riehle, and S. Grün, *Scientific Reports* **8**, 1 (2018).
- [89] S. DiSanto, P. Villegas, R. Burioni, and M. A. Munoz, *Proceedings of the National Academy of Sciences* **115**, E1356 (2018), ISSN 0027-8424, <http://www.pnas.org/content/early/2018/01/26/1712989115.full.pdf>.
- [90] A. K. Barreiro, J. N. Kutz, and E. Shlizerman, *The Journal of Mathematical Neuroscience* **7**, 10 (2017), ISSN 2190-8567.
- [91] M. Steriade, A. Nuñez, and F. Amzica, *J. Neurosci.* **13**, 3252 (1993).

- [92] A. Destexhe, S. W. Hughes, M. Rudolph, and V. Crunelli, *TINS* **30**, 334 (2007), ISSN 0166-2236, july INMED/TINS special issue—Physiogenic and pathogenic oscillations: the beauty and the beast.
- [93] P. C. Bressloff, *SIAM J. appl. math.* **70**, 1488 (2009).
- [94] P. C. Bressloff and O. Faugeras, *Journal of Statistical Mechanics: Theory and Experiment* **2017**, 033206 (2017).
- [95] A. Altland and B. Simons, *Concepts of Theoretical Solid State Physics* (Cambridge University Press, 2010).
- [96] C. Husemann and M. Salmhofer, *Phys. Rev. B* **79**, 195125 (2009).
- [97] N. Wentzell, G. Li, A. Tagliavini, C. Taranto, G. Rohringer, K. Held, A. Toschi, and S. Andergassen, arxiv preprint, arXiv:1610.06520 (2016).
- [98] C. J. Eckhardt, G. A. H. Schober, J. Ehrlich, and C. Honerkamp, *Phys. Rev. B* **98**, 075143 (2018).
- [99] B. A. W. Brinkman, F. Rieke, E. Shea-Brown, and M. A. Buice, arXiv preprint arXiv:1702.00865 (2017).
- [100] B. Bravi and P. Sollich, *Physical Biology* **14**, 045010 (2017).
- [101] M. M. e. a. Churchland, *Nat. Neurosci.* **13**, 369 (2010).
- [102] A. Litwin-Kumar, M. J. Chacron, and B. Doiron, *PLOS Comput. Biol.* **8**, e1002667 (2012).
- [103] M. Ohbayashi, K. Ohki, and Y. Miyashita, *Science* **301**, 233 (2003), ISSN 0036-8075, <http://science.sciencemag.org/content/301/5630/233.full.pdf>.
- [104] M. Henningson and S. Illes, *Front Comput Neurosci* **11** (2017).
- [105] M. Kardar, G. Parisi, and Y.-C. Zhang, *Phys. Rev. Lett.* **56**, 889 (1986).
- [106] K. J. Wiese, *Journal of Statistical Physics* **93**, 143 (1998), ISSN 1572-9613.
- [107] V. Priesemann, M. Wibral, M. Valderrama, R. Pröpper, M. Le Van Quyen, T. Geisel, J. Triesch, D. Nikolic, and M. H. J. Munk, **8**, 80 (2014), ISSN 1662-5137.
- [108] J. Wilting and V. Priesemann, *Nature communications* **9**, 2325 (2018).
- [109] P. Bak, C. Tang, and K. Wiesenfeld, *Phys. Rev. Lett.* **59**, 381 (1987).
- [110] L. Martignon, H. von Hasseln, S. Grün, A. Aertsen, and G. Palm, *Biol. Cybern.* **73**, 69 (1995).
- [111] E. Schneidman, M. J. Berry, R. Segev, and W. Bialek, *Nature* **440**, 1007 (2006).
- [112] T. Mora and W. Bialek, *Journal of Statistical Physics* **144**, 268 (2011), ISSN 1572-9613.
- [113] S. S. Manna, *Journal of Physics A: Mathematical and General* **24**, L363 (1991).

- [114] A. Vespignani, R. Dickman, M. A. Muñoz, and S. Zapperi, *Phys. Rev. Lett.* **81**, 5676 (1998).
- [115] R. Dickman, A. Vespignani, and S. Zapperi, *Phys. Rev. E* **57**, 5095 (1998).
- [116] P. Le Doussal and K. J. Wiese, *Phys. Rev. Lett.* **114**, 110601 (2015).
- [117] L. Canet, H. Chaté, and B. Delamotte, *J Phys. A* **44**, 495001 (2011).
- [118] M. A. Buice, J. D. Cowan, and C. C. Chow, *Neural Comput.* **22**, 377 (2010).
- [119] A. Andrianov, G. Biroli, J.-P. Bouchaud, and A. Lefevre, *Phys. Rev. E* **74**, 030101 (2006).
- [120] A. Lefevre and G. Biroli, *Journal of Statistical Mechanics: Theory and Experiment* **2007**, P07024 (2007).
- [121] O. Harish and D. Hansel, *PLoS Comput Biol* **11**, e1004266 (2015).
- [122] J. Schuecker, S. Goedeke, and M. Helias, *arXiv* (2017), 1603.01880v3 [q-bio.NC].
- [123] A. Crisanti and H. Sompolinsky, *arxiv preprint*, *arXiv:1603.08270* (2018).
- [124] A. Hawkes, *J. R. Statist. Soc. Ser. B* **33**, 438 (1971).
- [125] A. Hawkes, *Biometrika* **58**, 83 (1971).
- [126] G. K. Ocker, K. Josić, E. Shea-Brown, and M. A. Buice, *PLOS Computational Biology* **13**, 1 (2017).
- [127] M. A. Buice and C. C. Chow, *PLoS Comput Biol* **9**, 1 (2013).
- [128] S. Qiu and C. Chow, *arXiv preprint arXiv:1805.03601* (2018).
- [129] R. B. Stein, *Biophys. J.* **7**, 37 (1967).
- [130] R. Brette and W. Gerstner, *J. Neurophysiol.* **94**, 3637 (2005).
- [131] D. J. Amit and N. Brunel, *Cereb. Cortex* **7**, 237 (1997).